

Dielectric function of dense plasmas, their stopping power, and sum rules

Yu. V. Arkhipov, A. B. Ashikbayeva, A. Askaruly, and A. E. Davletov

Department of Physics and Technology, IETP, al-Farabi Kazakh National University, al-Farabi 71, 050040 Almaty, Kazakhstan

I. M. Tkachenko*

Instituto de Matemática Pura y Aplicada, Universidad Politécnica de Valencia, Camino de Vera s/n, 46022 Valencia, Spain

(Received 29 August 2014; published 14 November 2014; corrected 8 January 2015)

Mathematical, particularly, asymptotic properties of the random-phase approximation, Mermin approximation, and extended Mermin-type approximation of the coupled plasma dielectric function are analyzed within the method of moments. These models are generalized for two-component plasmas. Some drawbacks and advantages of the above models are pointed out. The two-component plasma stopping power is shown to be enhanced with respect to that of the electron fluid.

DOI: [10.1103/PhysRevE.90.053102](https://doi.org/10.1103/PhysRevE.90.053102)

PACS number(s): 52.25.Mq, 52.27.Aj

I. INTRODUCTION

The extension of numerous models for the description of the coupled or nonideal plasma dynamic properties onto the density-temperature domain characteristic of inertial fusion bound experiments [1] is a hot problem nowadays. In particular, the diagnostic methods applied in these experimental studies require a reliable method of reconstruction of the ion-ion dynamic structure factor and the method of moments [2–8] has demonstrated its advantages here with respect to other approaches recently [9]. What are these advantages based on? When we wish to enter the realm where the correlations between charged particles in a plasma become more and more important in comparison with the kinetic characteristics of the particles, when the system ceases to possess small parameters, how can we control the qualities of the model we develop?

We believe that sum rules can help us answer these questions and determine the level of accuracy of dynamic theories of nonperturbative systems [10]. Certainly, the f -sum rule related to the density conservation is a pillar of any such model, but there are other pillars. These are other conservation laws and higher-order sum rules. The latter take into account the correlations in the system under scrutiny and if the system dynamic characteristics, e.g., the dielectric function, do not satisfy these rules, which are effectively additional conservation laws, it is difficult to expect the corresponding model to be adequate in the strong-coupling domain. The advantage of the approach based on the theory of moments is that the constructed (inverse) dielectric function satisfies all sum rules taken into account automatically. The disadvantage is related to the necessity to model a phenomenologically unknown and immeasurable parameter function with certain mathematical properties, the Nevanlinna parameter function (NPF). The latter can be either reconstructed from available dynamic data, as done in [9] by the local constraints method (see [8] and references therein), or modeled on the basis of additional exact properties and/or limiting properties, as suggested in [11]. The point or the hope is that the main physical properties of the dynamic characteristic reconstructed on the basis of sum rules depend on the NPF model weakly.

As we will show, in one-component plasmas the random-phase approximation (RPA) with an adequate dynamic local-field correction complies with the higher-order sum rule, but in two-component plasmas it does not. On the other hand, the above dynamic models based on the Mermin extension [12] of the RPA do not help to take into account the system correlations even if all applicable conservation laws are included [13,14].

The scope of the work is the following. First we will see in detail whether the available different model expressions for the electron plasma dielectric function satisfy the sum rules, especially those related to the system coupling. Then we will generalize these models to two-component plasmas (TCPs) and demonstrate that in this case the correlation-related sum rule is not satisfied by these generalizations and that the dielectric function constructed within the method of moments has a significant advantage in this sense. The importance of the sum rules for the moderately and strongly coupled completely ionized plasma (polarization) stopping power will be analyzed as well, particularly in TCPs, where the electron-ion interaction within the target is shown to enhance the plasma stopping power. Certain conclusions will be finally drawn and some additional information will be provided in the Appendixes.

A. Loss function

Modeling of the dielectric function (DF) $\epsilon(k, \omega)$ or the inverse dielectric function (IDF) $\epsilon^{-1}(k, \omega)$ of strongly coupled Coulomb systems is actively discussed in the literature, in particular, because the corresponding loss function

$$\mathcal{L}(k, \omega) = -\text{Im} \epsilon^{-1}(k, \omega) / \omega \geq 0, \quad (1)$$

which is an even function of the real frequency ω , determines the polarization stopping power of such systems [15]. The non-negativity of the loss function stems from a similar property of $-\text{Im} \epsilon^{-1}(k, \omega)$ for positive frequencies, which in turn follows from the fluctuation-dissipation theorem since the (charge-charge) dynamic structure factor $S_{cc}(k, \omega)$ is non-negative by definition

$$\mathcal{L}(k, \omega) = \pi \beta \phi(k) b(\beta \hbar \omega) S_{cc}(k, \omega). \quad (2)$$

Here $\beta^{-1} = k_B T$ is the system temperature in energy units, k_B and \hbar are the Boltzmann and Planck constants, respectively,

*imtk@mat.upv.es

and $\phi(k) = 4\pi e^2/k^2$; the function $b(x) = [1 - \exp(-x)]/x$ is obviously strictly positive. We presume the system we consider to be in thermal equilibrium, uniform, and unmagnetized.

The analyticity of the prolongation of the IDF onto the upper half plane of the complex frequency $w = \omega + i\delta$, $\delta > 0$, is due to the causality principle and the Kramers-Kronig relations are always valid for this function:

$$\epsilon^{-1}(k, w) = 1 + \int_{-\infty}^{\infty} \frac{\text{Im} \epsilon^{-1}(k, \omega) d\omega}{\omega - w} \frac{1}{\pi}, \quad \text{Im } w > 0. \quad (3)$$

Additionally,

$$\epsilon^{-1}(k, 0) = \lim_{\delta \downarrow 0} \epsilon^{-1}(k, i\delta) = 1 + P \int_{-\infty}^{\infty} \text{Im} \epsilon^{-1}(k, \omega) \frac{d\omega}{\pi \omega}, \quad (4)$$

where P implies the principal value of the integral.

Consider the sum rules for the IDF, which are effectively the (non-negative) power moments of the loss function [4–8]:

$$C_l(k) = \frac{1}{\pi} \int_{-\infty}^{\infty} \omega^l \mathcal{L}(k, \omega) d\omega, \quad l = 0, 1, 2, \dots \quad (5)$$

The odd-order moments vanish due to the symmetry of the loss function.

The expression for the zeroth moment follows immediately from (4) since the loss function can be considered continuous at $\omega = 0$:

$$C_0(k) = -\frac{1}{\pi} \int_{-\infty}^{\infty} \frac{\text{Im} \epsilon^{-1}(k, \omega)}{\omega} d\omega = 1 - \epsilon^{-1}(k, 0) > 0. \quad (6)$$

The inequalities of the form

$$\epsilon^{-1}(k, 0) \leq 1 \iff \epsilon(k, 0) \geq 1, \quad \epsilon(k, 0) < 0 \quad (7)$$

also follow directly from (4) (see [16,17] and references therein); the values of $\epsilon(k, 0)$ between 0 and 1 turn out to be forbidden and the causality conditions corresponding to the action of the external charge on the system do not preclude negative values for a static DF of the system. If the static DF $\epsilon(k, 0)$ becomes negative, then the analyticity of the DF in the half plane $\text{Im } w > 0$ might break down.

We are interested here in taking into account not only the sum rules, but other exact relations as well. We wish to consider multispecies systems and the method of moments does not involve essentially the local-field corrections and expresses the dynamic properties in terms of the system static characteristics such as the static structure factors and the moments themselves. Therefore, we are not explicitly bounded, e.g., by the Niklasson condition or the compressibility sum rule [18,19], though the latter is important for the correct solution of the Ornstein-Zernicke equation; e.g., in the hypernetted approximation we use it to compute the system partial static structure factors. The exact relation that directly influences our expression for the TCP IDF is, along the Kramers-Kronig relations, the Perel'-Eliashberg exact asymptotic form [20] (particularly in a hydrogenlike two-component completely ionized plasma with the neutrality condition $n_e = Zn_i$)

$$\begin{aligned} \text{Im} \epsilon[k, \omega \gg (\beta\hbar)^{-1}] &\simeq A(\omega_p/\omega)^{9/2}, \\ A &= 3^{-5/4} \sqrt{2} Z r_s^{3/4}. \end{aligned} \quad (8)$$

The Brueckner parameter $r_s = a/a_B$ is determined by the electronic Wigner-Seitz radius $a = (3/4\pi n_e)^{1/3}$, $a_B = \hbar^2/m_e e^2$ is the Bohr radius, and $\omega_p = \sqrt{4\pi n_e e^2/m_e}$ is the (electronic) plasma frequency. At high frequencies the asymptotic forms of the DF and IDF differ only in sign, so the loss function behaves at high frequencies as $\omega^{-11/2}$. This implies that in a real system the sixth- and higher-even-order power moments must diverge. The result (8) was rediscovered in [21(a)]; see also [21(b)].

Observe also that due to the f -sum rule,

$$C_2 = \omega_p^2.$$

We will apply the method of moments to the set

$$\{C_0(k), 0, C_2, 0, C_4(k)\} \quad (9)$$

and use the characteristic frequencies

$$\begin{aligned} \omega_1(k) &= \sqrt{C_2/C_0(k)} = \omega_p / \sqrt{1 - \epsilon^{-1}(k, 0)}, \\ \omega_2(k) &= \sqrt{C_4(k)}/\omega_p. \end{aligned} \quad (10)$$

Note that due to the non-negativity of the loss function and the Cauchy-Schwarz inequality (see Appendix A) the above set of moments (9) is positive definite and thus the corresponding Hamburger moment problem of reconstruction of the loss function is solvable [2,3]. Since, due to (3), we can rewrite the IDF as

$$\epsilon^{-1}(k, w) = \epsilon^{-1}(k, 0) - \frac{w}{\pi} \int_{-\infty}^{\infty} \frac{\mathcal{L}(k, \omega) d\omega}{\omega - w}, \quad (11)$$

the Nevanlinna theorem and formula determine the noncanonical solutions of the Hamburger moment problem for the IDF as well (see Sec. III A).

It is important also that the explicit exact forms of these convergent moments can be derived independently of a particular DF or IDF model of an equilibrium plasma. The latter limitation can be avoided [22(a)] by applying the matrix version of the method of moments [22(b)] in the species space [22(c)].

The asymptotic expansion of the IDF along any ray in the upper half plane $\text{Im } w > 0$ can be easily constructed from (11):

$$\begin{aligned} \epsilon^{-1}(k, w \rightarrow \infty) &\simeq \epsilon^{-1}(k, 0) + \frac{1}{\pi} \int_{-\infty}^{\infty} \left[1 + \frac{\omega}{w} + \left(\frac{\omega}{w}\right)^2 + \dots \right] \mathcal{L}(k, \omega) d\omega \\ &= 1 + \frac{\omega_p^2}{w^2} + \frac{\omega_p^2 \omega_2^2(k)}{w^4} + \dots \end{aligned} \quad (12)$$

Similarly, if the dielectric function itself is a response function, i.e., if $\epsilon(k, 0) > 1$,

$$\epsilon(k, w \rightarrow \infty) \simeq 1 - \frac{\omega_p^2}{w^2} - \frac{\omega_p^2 [\omega_2^2(k) - \omega_p^2]}{w^4} + \dots, \quad (13)$$

so that for

$$\mathcal{P}(k, \omega) = \text{Im} \epsilon(k, \omega) / \omega, \quad (14)$$

which is also presumed to be non-negative and even for any real frequency ω ,

$$\begin{aligned} M_l(k) &= \frac{1}{\pi} \int_{-\infty}^{\infty} \omega^l \mathcal{P}(k, \omega) d\omega, \quad l = 0, 2, 4, \\ M_0(k) &= \epsilon(k, 0) - 1, \quad M_2 = \omega_p^2, \\ M_4(k) &= C_4(k) - C_2^2. \end{aligned} \quad (15)$$

Indeed, if

$$\begin{aligned} \epsilon(k, w) &= 1 + \frac{1}{\pi} \int_{-\infty}^{\infty} \frac{\text{Im} \epsilon(k, \omega)}{\omega - w} d\omega, \quad \text{Im} w > 0, \\ M_0(k) &= \frac{1}{\pi} \int_{-\infty}^{\infty} \frac{\text{Im} \epsilon(k, \omega)}{\omega} d\omega = \epsilon(k, 0) - 1; \end{aligned} \quad (16)$$

however, the positivity of the fourth moment $M_4(k)$ does not follow from the Cauchy-Schwarz inequality in L^2 (see Appendix A).

Hence, the coefficients of the asymptotic expansion of a certain function along any ray in the upper half plane coincide with the *convergent* power moments of the corresponding distribution density (the loss function in our case) only if we deal with a Nevanlinna function [2], i.e., with a response function. In general, there are no reasons for the loss function higher moments (for even $l > 4$) to diverge in one-component plasmas (OCPs), particularly in electron fluids, but we show that they do for some of the models we consider here. Due to the definition of an asymptotic expansion, such divergence does not mean that lower-order sum rules are not satisfied; such an option was not considered in [23].

In other words, in order to employ the Akhiezer theorem [3] to determine the quality of a model dynamic characteristic, e.g., the IDF (or the DF, if it is a response function), one has to study the convergence of the corresponding power moments and the high-frequency asymptotic expansion of the dynamic function in question. On the other hand, if we know that in a real Coulomb system higher-order even moments must diverge but in a certain model they do not, this can be considered as a drawback for this model.

B. Models

The long way to the current situation with the plasma DF or IDF modeling was initiated (in the long-wavelength limiting case) by the Drude-Lorentz model and developed by the RPA. The collisionless one-component (usually, electronic) Lindhard dielectric function [15] $\epsilon_{\text{RPA}}(k, \omega)$ was generalized by Mermin [12] and later by Das [24], who used an alternative distribution function variation method to take the collisions into account in the relaxation-time approximation. Note that the direct extension of the Lindhard dielectric function by replacing ω with $\omega + i\nu$, ν being the collision frequency, fails to conserve the local density [12].

Mathematical properties and different versions of the Lindhard DF were further considered in a number of elaborate studies. We point out the seminal paper of Gouedard and Deutsch [25] and the paper of Arista and Brandt [26], who managed to rewrite the RPA dielectric function in a way that, at least in the 1980s, was more suitable for calculations. The high-frequency asymptotic behavior of the Lindhard DF at

high and low temperatures was studied in [25,26] in detail. Recently, the Mermin model was extended to include, along the density conservation, the energy and momentum conservation laws [13,14]. On the other hand, the influence of these model IDFs on the plasma stopping power was thoroughly studied by Barriga-Carrasco and co-workers in a series of papers [27,28].

In our present work we study the asymptotic and analytic properties of the RPA, the Mermin DF, the extended Mermin DF, and the full conserving DF (FCDF). Precisely, from the point of view of the method of moments (MM) [2–8] discussed above and in Sec. III A in more detail, we wish to determine whether the sum rules (other than the f -sum rule) are satisfied by these models. The convergent fourth-order sum rule, which is the fourth frequency power moment of the loss function (1) $C_4(k)$, includes the correlation contributions and thus its fulfillment is presumably crucial for strongly coupled systems such as those of inertial fusion [1]. Note also that the long-wavelength limiting form of $C_4(k)$ related to the target electron-ion correlations modifies the well-known Bethe-Larkin logarithmic asymptotic form of the polarization stopping power of heavy ions in strongly coupled two-component plasmas [29] and we believe that if this fourth-moment sum rule does not hold for a certain DF model, the predictions of this model on the plasma stopping power should differ from those based on the MM and eventually from the real experimental data. What matters, from the point of view of an experimentalist, is to what extent they will differ and whether they will be observable.

Though the derivation of the Mermin dielectric function

$$\epsilon_{\text{M}}(k, \omega) = 1 + \frac{(\omega + i\nu)[\epsilon_{\text{RPA}}(k, \omega + i\nu) - 1]}{\omega + i\nu \frac{\epsilon_{\text{RPA}}(k, \omega + i\nu) - 1}{\epsilon_{\text{RPA}}(k, 0) - 1}} \quad (17)$$

guarantees the conservation of the local number of charged particles (electrons), this model is valid only in the first order in the total electrostatic potential energy and presumably cannot describe the properties of the plasma liquid phase at any value of the coupling parameter

$$\Gamma = \beta e^2 / a \quad (18)$$

and at any degeneracy. Nevertheless, it is actively employed under variable physical conditions (see, e.g., [27,30]).

On the other hand, the generalized Drude-Lorentz model for the IDF [31]

$$\epsilon_{\text{GDL}}^{-1}(0, \omega) = 1 + \frac{\omega_p^2}{\omega^2 - \omega_p^2 + i\omega\nu(\omega)} \quad (19)$$

is often used in numerical simulations of dense plasmas [31,32]. Note that the corresponding (internal) dynamic conductivity

$$\sigma^{\text{int}}(\omega) = \frac{\omega}{4\pi i} [\epsilon_{\text{GDL}}(0, \omega) - 1] = \frac{i\omega_p^2 / 4\pi}{\omega + i\nu(\omega)}$$

converts into the classical Drude-Lorentz model if we neglect the frequency dependence of the generalized (complex) collision frequency $\nu(\omega)$, the static conductivity being equal to $\omega_p^2 / 4\pi\nu(0)$.

The static collision frequency $\nu = \nu(0)$ is determined, e.g., by the Spitzer formula or in the general Green-Kubo context

[33]. The interpolation formula for the static conductivity [34] can be used for an initial evaluation.

The dynamic collision frequency, in hydrogenlike plasmas, can be introduced to take into account the ion-ion correlations in the Born approximation via the static ion-ion structure factor $S_{ii}(q)$ (see [30] and references therein),

$$\nu(\omega) = \frac{n_i}{6\pi^2 m_e^2} \int_0^\infty q^6 V_{ei}^2(q) S_{ii}(q) \times \frac{\epsilon_{\text{RPA},e}(q, \omega) - \epsilon_{\text{RPA},e}(q, 0)}{i\omega\omega_p^2} dq. \quad (20)$$

Here

$$V_{ei}(q) = -\frac{4\pi Z e^2}{q^2 \epsilon_{\text{RPA},e}(q, 0)}$$

is the statically screened electron-ion interaction potential. Note that (20) is obtained within the kinetic approach and it does not contain the electron-ion correlation contribution. The standard definition of the (electronic) DF in the RPA is provided in Sec. II.

A development of the topic has been suggested in [35], where, in a consistent way, the Mermin model for the dielectric function of electronic fluids at $T = 0$ has been extended to include the dynamic local-field correction (LFC) modeled in three different ways. We will also discuss the extensions of the Mermin model that include the dynamic collision frequency (20) (the Born-Mermin approximation) [35] or other conservation laws [13,14].

As we have mentioned, we wish to compare the above models to the IDF model based on the nonperturbative method of moments and valid at finite temperatures. Notice that the viscoelastic approximation [19,36] and the approach based on the continuous fractions [37] are particular cases of the MM [7].

As we have seen, the sum-rule conditions can be checked using the asymptotic expansions of the model expressions in question [3]. Other theoretical approaches can be treated in a similar way, e.g., the quasilocalized charge approximation [38] (see [39]).

It was stated in [23] (also using the asymptotic expansions but without referring to the method of moments) that for a one-component system the compressibility sum rule, the f -sum rule, and the loss function fourth-frequency-moment sum rule could be satisfied by the FCDF [13] only within the quasiparticle approach by taking into account the effective mass and self-energy, i.e., some unknown smooth functions. This approach has been generalized to multispecies systems for the (asymmetric) nuclear matter by introducing the matrix (in the species space) of non-Markovian, i.e., frequency-dependent, relaxation times related to the interspecies (transport) cross sections [40].

Like other theoretical approaches heavily dependent on the LFCs, for example [35], these results have not been extended to multispecies plasmas at nonzero temperatures. On the other hand, the application of the MM permits one to include, via the moments, the interspecies static correlations with the partial static structure factors evaluated, e.g., within the hypernetted-chain approach at $T \neq 0$, while usually the application of the local-field theory to multispecies systems

is based on the mixing rule, i.e., is carried out in the additive way. Certainly, the account of quantum-mechanical effects in the static characteristics is desirable.

To put our considerations on a more solid basis, we recall in Sec. II the definitions and results stemming from the causality, the sum rules, and the asymptotic expansions in strongly coupled one-component plasmas and outline the properties of the MM-generated IDF. Then we study the analytic prolongation $\epsilon_{\text{RPA}}(k, \omega + i\nu)$ of the Lindhard dielectric function at $\omega = \omega + i\nu \in \mathbb{C}$, $\nu > 0$, and its limiting form when $\nu \downarrow 0$ and do the same with the FCDF model of [13,14] as well. This prolongation has been performed in [35], but for $T = 0$ only, and it facilitates a correct application of the Mermin model expressions. We reduce the RPA DF in the upper half plane to the Arista-Brandt form [26] and determine to what extent the above models of the DF satisfy the sum rules. Then we carry out a comparison between the RPA and extended Mermin models for the electron fluid DF, including at finite temperature, and the MM-generated DF, extend these results to multispecies plasmas, and present some relevant numerical results.

Further, the repercussions of the above model constructions on the plasma stopping power (Sec. IC) are analyzed in Sec. IV. The differences between one- and two-component models are to be pointed out in this sense. For simplicity of notation and until Sec. III we consider one-component electron fluids and omit the species subscripts wherever possible.

C. Polarization stopping power

Measuring energy losses of beams of charged particles is an important diagnostic tool in both modern condensed matter and plasma physics. Bethe [41] derived a simplified formula for the stopping power that describes the energy losses of fast projectiles in a solid modeled as a system of quantum-mechanical oscillators. Later, Larkin [42] demonstrated that the analogous formula remains valid for fast but not relativistic ions permeating an electron gas,

$$-\frac{dE}{dx} \underset{v \rightarrow \infty}{\simeq} \left(\frac{Z_p e \omega_p}{v} \right)^2 \ln \frac{2m_e v^2}{\hbar \omega_p}, \quad (21)$$

in which the oscillator frequency is effectively replaced by the plasma frequency. Here $Z_p e$ and v stand for the electric charge and velocity of the projectile, respectively, and the electron gas is characterized by the number density n_e with m_e and $-e$ being the electron mass and charge, respectively.

Formula (21) is usually employed to determine the number density of electrons in a target traditionally treated experimentally as an electron fluid [43–45]. The x-ray Thomson scattering excepted, this technique remains the only suitable candidate for the diagnostics of hot and dense ($n_e \gtrsim 10^{19} \text{ cm}^{-3}$) plasmas [45] (see also [46] and references therein).

It was shown in [29] that in a two-component completely ionized hydrogen plasma with a weakly damped Langmuir mode of dispersion $\omega_L(k)$, the plasma frequency in the Coulomb logarithm of (21) should be replaced by the long-wavelength limiting value of $\omega_L(k)$, $\omega_L(0) = \omega_p \sqrt{1 + H}$ with $H = [g_{ei}(0) - 1]/3$, $g_{ei}(r)$ being the electron-ion radial distribution function, i.e., this correction is due to the interaction of the electrons with the target ions. It should be noted that

the generalization of [29] to partially ionized plasmas or plasmas with complex ions and a larger number of species is rather straightforward (see, e.g., [28,47,48]). At present, this electron-ion correlation correction to the electron fluid stopping power might not be observable due to a relatively low accuracy of the experimental techniques available, but for dicluster heavy-ion projectiles [49] that correlation correction could become more pronounced.

The problem of stopping power computing for relativistic projectiles has recently arisen due to the reported experiments with protons decelerating from velocities of up to 80% of the speed of light [50] (see also [51]). The importance of the relativistic corrections to the classical asymptotic form (21) of the stopping power as compared to the above intertarget electron-ion correlation contribution was estimated recently in [52]. In a partially ionized plasma the bound-electron contribution can be taken into account [47] by incorporating the ionization losses, but here the plasma is considered to be completely ionized. Such an assumption allows one to adopt the polarization picture to calculate the stopping power of a Coulomb system.

Lindhard [15] expressed the polarization stopping power in terms of the medium longitudinal dielectric function $\epsilon(k, \omega)$. This expression can further be generalized by applying the Fermi golden rule [53] to obtain [54–58]

$$\left(-\frac{dE}{dx}\right)^{\text{pol}} = -\frac{2(Z_p e)^2}{\pi \beta \hbar v^2} \int_0^\infty \frac{dk}{k} \int_{\alpha_-(k)}^{\alpha_+(k)} \frac{\text{Im} \epsilon^{-1}(k, \omega)}{b(\beta \hbar \omega)} d\omega, \quad (22)$$

where $\alpha_\pm(k) = \pm kv + \hbar k^2/2M(v)$ and $M(v)$ is the mass of the projectile with a speed v . What matters is that the above expression involves the target medium (inverse) dielectric function $\epsilon^{-1}(k, \omega)$, which is a genuine response function. Two essential physical restrictions are imposed by applying formula (22). First of all, no magnetization effects are taken into account, so the plasma dielectric function depends on the wave-vector modulus. Second, the interaction between the projectile and the plasma medium is treated in a linear approximation. Notice that, e.g., the Z_p^3 Barkas contribution to the stopping power [59] identically vanishes in a fully ionized plasma [60].

In the past, the polarization stopping power was quite extensively studied in the literature. The problem was thoroughly analyzed within the RPA [54,55,61–63] and beyond by introducing an analytical formula for the LFC [54,64–67], derived within the T -matrix approach [57,68], the method of effective potentials [69], or using the Mermin or more sophisticated models for the dielectric function [27] to name a few.

Though the coupling between the projectile and the target plasma is treated perturbatively, no further restriction is imposed here on the value of the plasma coupling parameter Γ . The only limitation left is that the plasma must remain in the liquidlike phase, although the modeling of its dielectric properties remains a sophisticated problem since its characteristic lengths, i.e., the Wigner-Seitz radius and the Debye length $\lambda_D = (4\pi n_e e^2 \beta)^{-1/2}$, are to be of the same order of magnitude. Note that in the nonideal plasma of interest herein, $\Gamma = a^2/3\lambda_D^2 \gtrsim 1$, which invalidates mean-field theories, such

as the RPA and other analogous perturbative approaches, and at the same time requires the electronic subsystem to be considered as degenerate.

If single-particle effects can be neglected (see, nevertheless, [54] for the corrections), the general expression for polarization losses simplifies as

$$\left(\frac{dE}{dx}\right)^{\text{pol}} = \frac{2}{\pi} \left(\frac{Z_p e}{v}\right)^2 \int_0^\infty \frac{dk}{k} \int_0^{kv} \omega \text{Im} \left(\frac{-1}{\epsilon(k, \omega)}\right) d\omega. \quad (23)$$

As we have mentioned, in a two-component plasma the asymptotic form (21) is modified [29] as

$$\left(-\frac{dE}{dx}\right)^{\text{pol}} \underset{v \rightarrow \infty}{\simeq} \left(\frac{Z_p e \omega_p}{v}\right)^2 \ln \frac{2m_e v^2}{\hbar \omega_p \sqrt{1+H}}, \quad (24)$$

where

$$H = \frac{1}{6\pi^2 \sqrt{n_e n_i}} \int_0^\infty p^2 S_{ei}(p) dp \quad (25)$$

is determined by the long-wavelength asymptotic value of the (TCP) loss function fourth frequency moment

$$H = \lim_{k \rightarrow 0} \left(\frac{1}{\pi \omega_p^4} \int_{-\infty}^\infty \omega^4 \mathcal{L}(k, \omega) d\omega - 1 \right).$$

The correlation correction is important when the electron-ion correlations do matter, i.e., when the plasma coupling parameter $\Gamma \gtrsim 1$. The partial static structure factors $S_{ab}(p)$ can be computed independently, e.g., by the method of hypernetted chains taking the correlations (but not the quantum effects) into account [70].

A semiquantitative estimate for the correction (25) was obtained in a modified RPA that interpolates the long- and short-wavelength asymptotic forms of the static polarization operator of a hydrogenlike plasma with $n_e = Zn_i$ [71]:

$$H_1 = \frac{4}{3} Z r_s \sqrt{\Gamma} [3Z\Gamma^2 + 4r_s + 4\Gamma \sqrt{3(1+Z)r_s}]^{-1/2}. \quad (26)$$

In weakly coupled plasmas with $\Gamma \rightarrow 0$, $H_1 \simeq (2Z/3)\sqrt{r_s \Gamma}$.

II. ELECTRON FLUID DF ASYMPTOTIC EXPANSION AND SUM RULES

A. Zeroth moment in the RPA, Mermin approximation, and FCDF approximation

The relation of the loss function zeroth moment to the static value of the plasma IDF is applicable to systems with an arbitrary number of components. Within the RPA the static dielectric function is defined as

$$\epsilon_{\text{RPA}}(k, 0) = 1 + \frac{4}{\pi a_B k^3} \int_0^\infty p f_{\text{FD}}(p) \ln \left| \frac{k/2 + p}{k/2 - p} \right| dp.$$

Here

$$f_{\text{FD}}(\mathbf{p}) = f_{\text{FD}}(p) = \{\exp[\beta E(p) - \eta] + 1\}^{-1}$$

is the Fermi-Dirac distribution density with $E(\mathbf{p}) = E(p) = \hbar^2 p^2/2m$. The dimensionless chemical potential $\eta = \beta \mu$ is

defined by the normalization equation $F_{1/2}(\eta) = 2D^{3/2}/3$ with

$$F_\nu = \int_0^\infty \frac{x^\nu dx}{\exp(x - \eta) + 1},$$

$$D = \beta E_F = \beta m v_F^2 / 2 = \beta \hbar^2 k_F^2 / 2m$$

$$= \beta \hbar^2 (3\pi^2 n)^{2/3} / 2m, \quad (27)$$

where $F_\nu(\eta)$, E_F , v_F , and k_F are the ν th-order Fermi integral, Fermi energy, velocity, and wave number, respectively.

In the Mermin approximation $\epsilon_M(k, \omega = 0) = \epsilon_{\text{RPA}}(k, 0)$, i.e., the zeroth sum rule is not satisfied since the real static IDF $\epsilon^{-1}(k, 0)$ takes the correlations into account while $\epsilon_{\text{RPA}}(k, 0)$ does not. Indeed, by virtue of the fluctuation-dissipation theorem,

$$\epsilon^{-1}(k, 0) = 1 - \beta \phi(k) \int_{-\infty}^{\infty} b(\beta \hbar \omega) S(k, \omega) d\omega.$$

In particular, in the classical approximation with $\hbar \rightarrow 0$,

$$\epsilon^{-1}(k, 0) = 1 - (k_D^2 / k^2) S(k). \quad (28)$$

Here $k_D^2 = 4\pi n e^2 \beta$, $S(k, \omega)$ is the (charge-charge) dynamic structure factor, and

$$S(k) = \frac{1}{n} \int_{-\infty}^{\infty} S(k, \omega) d\omega$$

is the system static structure factor (SSF).

It is easy to observe that within the FCDF model [see [27(d)]],

$$\epsilon_{\text{FC}}(k, \omega) = 1 + \phi(k) \frac{\Pi_0 + E}{1 + F}, \quad (29)$$

we still have that $\epsilon_{\text{FC}}(k, \omega = 0) = \epsilon_{\text{RPA}}(k, 0)$. Here

$$\Pi_\mu(k, w) = 2 \int \frac{d\mathbf{p} |\mathbf{p}|^\mu}{(2\pi)^3} \frac{f_{\text{FD}}(\mathbf{p} + \mathbf{k}/2) - f_{\text{FD}}(\mathbf{p} - \mathbf{k}/2)}{\hbar w - [E(\mathbf{p} + \mathbf{k}/2) - E(\mathbf{p} - \mathbf{k}/2)]},$$

$$B_\mu(k) = -\Pi_\mu(k, w = 0),$$

$$D_\mu(k, \omega) = (i\nu \Pi_\mu - \omega B_\mu) / w,$$

$$E(k, \omega) = \frac{-i\nu \Pi_2 \Pi_2 B_0 - \Pi_0 B_2}{w D_4 B_0 - B_2 D_2},$$

$$F(k, \omega) = \frac{i\nu \left(\frac{D_2 \Pi_2 - D_4 \Pi_0 - i\xi \Pi_2 (\Pi_2 B_0 - \Pi_0 B_2)}{D_4 B_0 - B_2 D_2} - 1 \right)}{w} + i\xi \Pi_0,$$

and $\xi = \omega \nu m / n k^2$. In particular,

$$\Pi_0(k, w) := \Pi(k, w)$$

$$= 2 \int \frac{d\mathbf{p}}{(2\pi)^3} \frac{f_{\text{FD}}(\mathbf{p} + \mathbf{k}) - f_{\text{FD}}(\mathbf{p})}{\hbar w - E(\mathbf{p} + \mathbf{k}) + E(\mathbf{p})} \quad (30)$$

is the (retarded) polarization operator (a simple loop) determined as in [72] (see Sec. IIB1). In Sec. VA we estimate the values of the zeroth moment in different approximations and show that they are in agreement with the above results.

For reference, we provide here an exact explicit expression for the fourth moment. In a coupled electron fluid (see [4–6, 6–8, 73] and references therein)

$$C_4^{\text{OCP}}(k) = \omega_p^4 [1 + W_0(k)] \quad (31)$$

and the correction of the fourth moment contains only two contributions

$$W_0(k) = V(k) + U(k). \quad (32)$$

The first contribution is produced by the kinetic term of the system Hamiltonian. In the classical case, $V(k)$ coincides with the well-known Vlasov contribution to the dispersion relation $V(k) = 3k^2/k_D^2$. In a degenerate system

$$V(k) = \frac{\langle v_e^2 \rangle k^2}{\omega_p^2} + \left(\frac{\hbar}{2m} \right)^2 \frac{k^4}{\omega_p^2}, \quad (33)$$

where the average of the square of the (electron) velocity is expressed as $\langle v_e^2 \rangle = 3F_{3/2}(\eta)/m\beta D^{3/2}$. The second contribution to the fourth moment stems from the interaction contribution to the system Hamiltonian

$$U(k) = \frac{1}{2\pi^2 n} \int_0^\infty p^2 [S(p) - 1] f(p, k) dp, \quad (34)$$

where we have introduced the angular factor

$$f(p, k) = \frac{5}{12} - \frac{p^2}{4k^2} + \frac{(k^2 - p^2)^2}{8pk^3} \ln \left| \frac{p+k}{p-k} \right|.$$

To describe experimental and simulation data within the moment approach, one should specify the characteristic frequencies (10) and the Nevanlinna parameter function (see below, Sec. III A, and [4–6, 6–8]). However, to apply the Mermin approximation, one first has to study other construction elements of (17).

B. The RPA DF analytic prolongation onto the upper half plane

1. Polarization operator

By definition

$$\epsilon_{\text{RPA}}(k, w) = 1 + \phi(k) \Pi(k, w). \quad (35)$$

Let us now reduce (30) to the convenient Arista-Brandt form [26]. Notice that the static polarization operator

$$\Pi(k, 0) = \frac{m}{\pi^2 \hbar^2 k} \int_0^\infty q f_{\text{FD}}(q) \ln \left| \frac{k+2q}{k-2q} \right| dq > 0 \quad (36)$$

and when $k \rightarrow 0$,

$$\Pi(k \rightarrow 0, 0) = \frac{m}{\pi^2 \hbar^2} \int_0^\infty f_{\text{FD}}(q) dq.$$

2. The Arista-Brandt form of the DF

The analytic extension of the well-known and generally employed expression for the polarization operator $\Pi(k, \omega)$ on the real axis [26] can be obtained by direct calculation

$$\Pi(k, w) = \Pi_0(k, \omega)$$

$$= \frac{3mn}{4z \hbar^2 k_F^2} [G_1(\sigma_1) - G_1(\sigma_2)], \quad \text{Im } w \geq 0. \quad (37)$$

Similarly, for other construction elements of the FCDF, we have obtained the following necessary prolongations onto the

upper half plane:

$$\begin{aligned} \Pi_2(k, w) = & \frac{mn}{\hbar^2} \left(\frac{2 + 3z[G_1(\sigma_1) - G_1(\sigma_2)]}{4} \right. \\ & - \frac{3[\sigma_1 G_1(\sigma_1) + \sigma_2 G_1(\sigma_2)]}{2} \\ & \left. + \frac{3[G_3(\sigma_1) - G_3(\sigma_2)]}{4z} \right), \end{aligned} \quad (38)$$

$$\begin{aligned} \Pi_4(k, w) &= \frac{mnk_F^2}{\hbar^2} \left[2 \left(\frac{3F_{3/2}(\eta)}{D^{5/2}} - 2zu \right) \right. \\ &+ \frac{3}{4z} [G_5(\sigma_1) - G_5(\sigma_2)] + \frac{3}{2} \{ 3z[G_3(\sigma_1) - G_3(\sigma_2)] \\ &- 3[\sigma_1 G_3(\sigma_1) + \sigma_2 G_3(\sigma_2)] + \frac{3z^3}{4} [G_1(\sigma_1) - G_1(\sigma_2)] \\ &- 3z[\sigma_1^2 G_1(\sigma_1) - \sigma_2^2 G_1(\sigma_2)] \\ &\left. - 3z^2[\sigma_1 G_1(\sigma_1) + \sigma_2 G_1(\sigma_2)] \right]. \end{aligned} \quad (39)$$

Here

$$\begin{aligned} G_l(\sigma) &= \int_0^\infty \frac{y^l dy}{\exp(Dy^2 - \eta) + 1} \ln \frac{\sigma + y}{\sigma - y}, \\ l = 1, 3, 5, \quad \text{Im } \sigma &\geq 0 \end{aligned} \quad (40)$$

and the expression (37) is that for the real part of $\Pi(k, \omega)$ but with the extended argument of the logarithmic integrand factor and with

$$\begin{aligned} u &= \frac{\omega}{kv_F} \rightarrow \frac{w}{kv_F} = \frac{\omega + i\nu}{kv_F} = u + i\gamma, \\ \sigma_{1,2} &= \frac{w}{kv_F} \pm z, \quad z = \frac{k}{2k_F}. \end{aligned}$$

Observe that when $\beta^{-1} \rightarrow 0$, (37) reduces to the zero-temperature form of the polarization operator obtained in [35]:

$$\lim_{\beta \rightarrow \infty} H_1(\sigma) = \sigma + \frac{1}{2}(1 - \sigma^2) \ln \frac{\sigma + 1}{\sigma - 1}. \quad (41)$$

Note also that any branch of the complex logarithm function can be used in (40) and (41).

3. Limiting properties

Certainly, when $\gamma \downarrow 0$, we return to the standard form of the polarization operator or the dielectric function [26]. For the real part of (37) this transition is obvious and for the imaginary part, due to the Dirac formula, we have

$$\begin{aligned} \text{Im } \Pi(k, \omega + i\nu) &= 2 \text{Im} \int \frac{d\mathbf{p}}{(2\pi)^3} \frac{f_{\text{FD}}(\mathbf{p} + \mathbf{k}) - f_{\text{FD}}(\mathbf{p})}{\hbar\omega + i\hbar\nu - E(\mathbf{p} + \mathbf{k}) + E(\mathbf{p})} \\ &= J(u + z) - J(u - z), \end{aligned} \quad (42)$$

where we have introduced the auxiliary function

$$\begin{aligned} J(x) &= \frac{mk_F^2}{2\pi\hbar^2k} \int_0^\infty \frac{y^2 dy}{\exp(Dy^2 - \eta) + 1} \int_{-1}^{+1} \delta(x - ys) ds \\ &= \frac{mk_F^2}{4\pi D\hbar^2k} \ln[\exp(\eta - Dx^2) + 1]. \end{aligned}$$

Note that only one of the Dirac δ functions can contribute in (42). Hence, since

$$\begin{aligned} \lim_{\eta \downarrow 0} \ln \left(\frac{x + i\gamma + y}{x + i\gamma - y} \right) &= \ln \left| \frac{x + y}{x - y} \right| - 2i\pi y \delta(x^2 - y^2), \\ \text{Im } \epsilon_{\text{RPA}}(k, \omega) &= \frac{k_F^2}{Dk^3 a_B} \ln \left(\frac{\exp[\eta - D(u - z)^2] + 1}{\exp[\eta - D(u + z)^2] + 1} \right). \end{aligned}$$

Finally, the classical form of the polarization operator in terms of the plasma dielectric function [74,75] is recovered when $\hbar \rightarrow 0$.

C. Higher-order sum rules

In this section we study the nonzero power moments of the OCP model dielectric functions named in the Introduction.

1. The RPA dielectric function

Consider, first, for the reference and for $\text{Im } w \geq 0$,

$$\begin{aligned} \epsilon_{\text{RPA}}(k, w) &= 1 + \frac{1}{4\pi a_B k_F} \left(\frac{2k_F}{k} \right)^3 \left[G_1 \left(\frac{w}{kv_F} + \frac{k}{2k_F} \right) \right. \\ &\quad \left. - G_1 \left(\frac{w}{kv_F} - \frac{k}{2k_F} \right) \right]. \end{aligned} \quad (43)$$

When $w \rightarrow \infty$ along any ray in the upper half plane,

$$\begin{aligned} &\left[G_1 \left(\frac{w}{kv_F} + \frac{k}{2k_F} \right) - G_1 \left(\frac{w}{kv_F} \right) \right] \\ &- \left[G_1 \left(\frac{w}{kv_F} - \frac{k}{2k_F} \right) - G_1 \left(\frac{w}{kv_F} \right) \right] \\ &\simeq 2G_1' \left(\frac{w}{kv_F} \right) \left(\frac{k}{2k_F} \right) + \frac{1}{3} G_1''' \left(\frac{w}{kv_F} \right) \left(\frac{k}{2k_F} \right)^3 + \dots \end{aligned}$$

The derivatives of $G_1(\sigma)$ can be easily calculated to give

$$\begin{aligned} \epsilon_{\text{RPA}}(k, w \rightarrow \infty) &\simeq 1 - \frac{\omega_p^2}{w^2} \left[1 + A_2(k) \left(\frac{kv_F}{w} \right)^2 \right. \\ &\quad \left. + A_4(k) \left(\frac{kv_F}{w} \right)^4 + O \left(\left(\frac{kv_F}{w} \right)^6 \right) \right], \end{aligned} \quad (44)$$

where [26] [using (33) and (27)]

$$\begin{aligned} A_2(k) &= \frac{3}{2} \frac{F_{3/2}(\eta)}{D^{5/2}} + \frac{\hbar^2 k^2}{4m_e^2 v_F^2} = \frac{\omega_p^2}{k^2 v_F^2} V(k), \\ A_4(k) &= \frac{3}{2} \frac{F_{5/2}(\eta)}{D^{7/2}} + \frac{\hbar^2 k^2}{4m_e^2 v_F^2} \frac{5F_{3/2}(\eta)}{D^{5/2}} + \frac{15}{4} \frac{\hbar^4 k^4}{m_e^4 v_F^4}, \dots \end{aligned}$$

Asymptotically, we have

$$\epsilon_{\text{RPA}}(k, w \rightarrow \infty) \simeq 1 - \frac{\omega_p^2}{w^2} \left(1 + \frac{\omega_p^2}{w^2} V(k) + \dots \right). \quad (45)$$

We conclude that, as expected, within the RPA the sum rule (31) is satisfied only partially, without taking the correlation contribution $U(k)$ into account.

2. Mermin dielectric function

Static collision frequency. The Mermin loss function satisfies the f -sum rule by construction. The situation with the fourth sum rule is quite different. It is not very difficult to calculate the high-frequency limit of the fourth-power-moment integrand to see that if the collision frequency is kept constant,

$$\lim_{\omega \rightarrow \infty} \left(- \frac{\omega^3 \text{Im} \epsilon_M^{-1}(k, \omega)}{\omega_p^3} \right) = \frac{\nu}{\omega_p},$$

which means that in the classical Mermin approximation (17) the fourth power moment of the loss function diverges and the corresponding sum rule (31) is not satisfied at all. In other words, the asymptotic expansion of the Mermin model DF with a constant collision frequency is just $\epsilon_M(k, w \rightarrow \infty) \simeq 1 - \omega_p^2/w^2$.

This behavior takes place because at high frequencies the imaginary part of the Mermin DF is determined by the imaginary part of the product $(1 + i\nu/\omega)[\epsilon_{\text{RPA}}(k, \omega + i\nu) - 1]$ and is reduced to the fractional form $-\nu\omega_p^2/\omega^3$, which significantly differs from the corresponding exponential factor characteristic for the RPA. This latter factor with the zero asymptotic expansion guarantees the convergence of all power moments of the RPA loss function to their collisionless values, while in the Mermin approximation only the second power moment survives.

Dynamic collision frequency. Consider the Born-Mermin approximation introduced in [35], i.e., the generalization of the Mermin model with the dynamic collision frequency included. We know that if the dielectric function is a response function, from (13) we have, for the electronic liquid,

$$\epsilon_e(k, w \rightarrow \infty) \simeq 1 - \frac{\omega_p^2}{w^2} - \frac{\omega_p^2 \Omega^2}{w^4} - \dots, \quad (46)$$

where

$$\Omega^2 = \omega_2^2(k) - \omega_p^2 = \omega_p^2 W_0(k) = \omega_p^2 [V(k) + U(k)], \quad (47)$$

with the same kinetic contribution (33), but with the correlation corrections $U(k)$ (34) present. On the other hand, in the RPA, from (44)

$$\epsilon_{\text{RPA}}(k, w \rightarrow \infty) \simeq 1 - \frac{\omega_p^2}{w^2} - \frac{\omega_p^2 \Omega_{\text{RPA}}^2}{w^4} - \frac{\omega_p^2 \Upsilon_{\text{RPA}}^4}{w^6} - O\left(\left(\frac{kv_F}{w}\right)^8\right) \dots, \quad (48)$$

with

$$\begin{aligned} \Omega_{\text{RPA}}^2 &= (kv_F)^2 A_2(k) = \omega_p^2 V(k), \\ \Upsilon_{\text{RPA}}^4 &= (kv_F)^4 A_4(k), \dots \end{aligned} \quad (49)$$

Hence, the asymptotic expansion of the dynamic collision frequency (20) imaginary part takes the following form:

$$\text{Im} \nu(\omega \rightarrow \infty) \simeq \frac{i\nu_1}{\omega} + O\left(\frac{i}{\omega^3}\right) + \dots,$$

with

$$\nu_1 = \frac{n_i}{6\pi^2 m_e^2 \omega_p^2} \int_0^\infty q^6 V_D^2(q) S_{ii}(q) [\epsilon_{\text{RPA},e}(q, 0) - 1] dq. \quad (50)$$

Thus, in the Born-Mermin (BM) approximation with the dynamic collision frequency $\nu(\omega)$ defined as in [30] (see also the references therein),

$$\epsilon_{\text{BM}}(k, w \rightarrow \infty) \simeq 1 - \frac{\omega_p^2}{w^2} - \frac{\omega_p^2 \Omega_{\text{BM}}^2}{w^4} - O\left(\frac{1}{w^6}\right),$$

where

$$\Omega_{\text{BM}}^2 = \Omega_{\text{RPA}}^2 + \nu_1 \neq \Omega^2, \quad (51)$$

which of course does not include the correlation corrections. It is important that, as established in [21], within the Born-Mermin approximation the real part of the collision frequency at high frequencies tends to zero as $\omega^{-3/2}$ and thus the corresponding loss function has only the second correct and the fourth incorrect convergent power moments (see Sec. V A). It is important also that the electronic fluid correlation correction $U(k)$ depends on the static structure factor $S_{ee}(q)$, while the ion-ion SSF $S_{ii}(q)$ would appear in the expression for the TCP fourth moment only in the first order in m_e/m_i , m_i being the ion mass [4–8].

D. Extended RPA and Mermin approximation

The extended Mermin approximation was suggested in [27(b)] and [35]. The extension consists in the introduction into the RPA dielectric function $\epsilon_{\text{RPA}}(k, w)$ of the dynamic local-field correction (DLFC),

$$\epsilon_{\text{XRPA}}(k, w) = 1 + \frac{\phi(k)\Pi(k, w)}{1 - \phi(k)G(k, \omega)\Pi(k, w)}, \quad (52)$$

$$\epsilon_{\text{XRPA}}(k, 0) = 1 + \frac{\phi(k)\Pi(k, 0)}{1 - \phi(k)G(k)\Pi(k, 0)}, \quad (53)$$

where $G(k) = G(k, \omega = 0)$ is the static local-field correction (SLFC), so that the extended Mermin dielectric function takes the following form:

$$\epsilon_{\text{XBM}}(k, \omega) = 1 + \frac{w\phi(k)\Pi(k, w)\Pi(k, 0)}{\omega\Pi(k, 0)[1 - \phi(k)G(k, w)\Pi(k, w)] + i\nu(\omega)\Pi(k, w)[1 - \phi(k)G(k)\Pi(k, 0)]}. \quad (54)$$

General properties and in particular the asymptotic expansion of the DLFC were studied in detail by Kugler [73]. At least, within the interpolation model for the DLFC approximation [67] employed in [35], the odd-order power moments of the DLFC diverge while the even-order moments vanish:

$$G(k, w) = G(k, \infty) + \frac{1}{\pi} \int_{-\infty}^{\infty} \frac{\text{Im } G(k, \omega)}{\omega - w} d\omega \underset{w \rightarrow \infty}{\simeq} G(k, \infty). \quad (55)$$

The latter characteristic, in electron fluids without the self-energy and effective mass corrections [23], equals $-U(k)$ [7,19] (see Appendix B). In our calculations we have employed the SLFC model suggested in [76].

Consider now the asymptotic expansion of the extended RPA dielectric function

$$\epsilon_{\text{XRPA}}(k, w \rightarrow \infty) \simeq 1 - \frac{\omega_p^2}{w^2} - \frac{\omega_p^2 \Omega^2}{w^4} - O\left(\frac{1}{w^6}\right), \quad \text{Im } w \geq 0,$$

which coincides with (46), i.e., the extended RPA dielectric function (if it is a response function), and satisfies the second and the fourth sum rules, while the corresponding function (14) satisfies the moment conditions (15). Moreover, the corresponding electron fluid IDF, which is always a response function, satisfies, as long as the static DF or the SSF is correct, all three nonzero convergent sum rules (5).

The extended Mermin approximation loses this advantage of the RPA. Precisely, if the collision frequency is considered constant, as in [27(b)], still the extended Mermin approximation DF does not satisfy the fourth sum rule independently of the form of the DLFC considered in this work or in [35]. Nevertheless, in the extended Born-Mermin approximation the fourth power moment converges, but we obtain the following expansion for the DF:

$$\epsilon_{\text{XBM}}(k, w \rightarrow \infty) \simeq 1 - \frac{\omega_p^2}{w^2} - \frac{\omega_p^2(\Omega^2 + \nu_1)}{w^4} - O\left(\frac{1}{w^6}\right), \quad \text{Im } w \geq 0. \quad (56)$$

We might say that the frequency-dependent collision frequency spoils the ability of the Born-Mermin model DF to satisfy the fourth sum rule. The above results on the OCPs are corroborated by the numerical results provided in Sec. V A.

E. The FCDF model

The FCDF model has not been extended in the above sense yet and one can observe, using the prolongations (38) and (39), that the asymptotic expansion of $\epsilon_{\text{FC}}(k, w)$ coincides with that of the RPA DF (48). We point out that the OCP stopping power computed in [27(d)] in the FCDF approximation is practically indistinguishable from that calculated in the RPA. In Sec. IV we will also see to what extent other details discussed in this section influence the plasma stopping power.

III. TWO-COMPONENT PLASMAS

Let us generalize now the above results to TCPs (multi-component plasma characteristics can be described in a similar way).

A. Moment approach

The asymptotic form (8) explicitly implies that in two-component or multicomponent plasmas the loss function power moments of even order higher than four diverge though the odd-order moments vanish. Thus, within the MM approach we consider now the same moment set (9), but with the moments specified for the system under consideration. This set is still positive definite, the corresponding (Hamburger) moment problem is solvable, and the condition of non-negativity of the corresponding loss function is also guaranteed. We will benefit from the advantage of this method: The corresponding expression for the IDF satisfies the sum rules automatically and it is applicable for any coupling or degeneracy in a liquid Coulomb system until crystallization takes place.

The moment problem corresponding to the TCP set $\{C_0(k), 0, C_2, 0, C_4(k)\}$ possesses [2,3] two families of solutions: the canonical and noncanonical solutions. A canonical solution of the moment problem has the form of a linear combination of weighted Dirac δ functions similar to the Feynman model for the liquid dynamic structure factor and provides good insight into the system dynamic properties [77]. Precisely the specific canonical solution of the moment problem

$$\frac{\mathcal{L}(k, \omega)}{\pi C_0(k)} = \frac{\omega_2^2(k) - \omega_1^2(k)}{\omega_2^2(k)} \delta(\omega) + \frac{\omega_1^2(k)}{2\omega_2^2(k)} [\delta(\omega - \omega_2(k)) + \delta(\omega + \omega_2(k))] \quad (57)$$

was employed in [29] to find the correction to the Bethe-Larkin stopping power asymptotic form and in [52] to estimate the relativistic corrections to the hydrogenlike nonideal plasma stopping power, which we have referred to above. From the physical point of view, the canonical solution describes nondecaying diffusive and Langmuir collective modes.

Noncanonical continuous solutions of the moment problem have been constructed in a number of publications (for mathematical details see [4–8], references therein, and also [39,78]). They can be easily obtained from the Nevanlinna theorem, which establishes a biunivocal correspondence between these solutions, particularly all (integrable) non-negative functions $\mathcal{L}(k, \omega)$ that possess the given moments $\{C_0(k), 0, C_2, 0, C_4(k)\}$ defined as in (5) (for $\kappa = 2$),

$$C_l(k) = \frac{1}{\pi} \int_{-\infty}^{\infty} \omega^l \mathcal{L}(k, \omega) d\omega := \langle \omega^l, 1 \rangle, \quad l = 0, 1, \dots, 2\kappa, \quad \kappa = 0, 1, 2, \dots, \quad (58)$$

and a set of NPFs $Q_\kappa(k, w)$,

$$\frac{1}{\pi} \int_{-\infty}^{\infty} \frac{\mathcal{L}(k, \omega)}{w - \omega} d\omega = \left\langle \frac{1}{w - \omega}, 1 \right\rangle = \frac{E_{\kappa+1} + Q_\kappa E_\kappa}{D_{\kappa+1} + Q_\kappa D_\kappa}. \quad (59)$$

The coefficients of the fractional-linear transformation of the NPF in (59) are orthogonal polynomials with exceptionally real and alternating zeros completely defined by the moments;

they can be easily constructed from the canonical basis of polynomials $\{1, \omega, \omega^2, \omega^3, \dots\}$ by the Gram-Schmidt procedure

$$\begin{aligned} D_0 &= 1, & D_1 &= \omega, & D_2 &= (\omega^2 - \omega_1^2), \\ D_2 &= \omega(\omega^2 - \omega_2^2), \\ E_\kappa(w) &= \left\langle \frac{D_\kappa(k, \omega) - D_\kappa(k, w)}{\omega - w}, 1 \right\rangle, \\ E_0 &= 0, & E_1 &= C_0(k), & E_2(\omega) &= \omega C_0(k), \\ E_3(\omega) &= \langle \omega^2 + \omega w + w^2 - \omega_2^2, 1 \rangle \\ &= C_2(k) + (w^2 - \omega_2^2)C_0(k). \end{aligned}$$

We have that

$$\begin{aligned} \langle D_\kappa, D_{\kappa'} \rangle &= \|D_\kappa\|^2 \delta_{\kappa\kappa'}, \\ \langle E_\kappa, E_{\kappa'} \rangle &= \|E_\kappa\|^2 \delta_{\kappa\kappa'}, \quad \kappa, \kappa' = 0, 1, 2, 3. \end{aligned}$$

The NPF $Q_\kappa(k, w)$ for any truncated moment problem of reconstruction of a response function that satisfies $2\kappa + 1$ sum rules $\{C_0, 0, C_2, 0, \dots, C_{2\kappa}\}$, as well as the response function, e.g., the IDF, belongs to the Nevanlinna class of functions (i.e., it is analytic in the half plane $\text{Im } w > 0$ and possesses there a non-negative imaginary part) and, additionally, it is such that in the same half plane and along any ray

$$\lim_{w \rightarrow \infty} Q_\kappa(k, w)/w = 0. \quad (60)$$

By virtue of the latter property of $Q_\kappa(k, w)$, the loss function $\mathcal{L}(k, \omega)$ and thus also the response function $\epsilon^{-1}(k, \omega)$ satisfy the sum rules (9) irrespectively of our choice of the parameter function $Q_\kappa(k, w)$, but this cannot be said *a priori* about the model expressions considered in Sec. IB.

I. Five-moment model

The sixth, divergent moment in the norm $\|D_3\|$ is the so-called immaterial element of the set $\{C_0(k), 0, C_2, 0, C_4(k)\}$; it does not prevent us apply the Nevanlinna formula (59). Indeed, for the above set of loss function moments (9), it stems from the Kramers-Kronig relations (3) that, due to this formula [6–8],

$$\begin{aligned} \epsilon_{\text{MM2}}^{-1}(k, w) - 1 &= w \frac{E_3 + Q_2 E_2}{D_3 + Q_2 D_2} - C_0(k) \\ &= \frac{\omega_p^2 [w + Q_2(k, w)]}{w(w^2 - \omega_2^2) + Q_2(k, w)(w^2 - \omega_1^2)}, \\ \text{Im } w &\geq 0, \end{aligned} \quad (61)$$

and this latter expression permits us to include the decay processes into consideration via the NPF. For any NPF of the above mathematical class any solution of the truncated moment problem $\{C_0(k), 0, C_2, 0, C_4(k)\}$ possesses all five convergent power moments of the given set by construction (see Sec. VA for numerical details). In addition, by virtue of the condition (60), i.e., without violating the sum rules, in a two-component plasma we can make use of the exact asymptotic form (8) of the DF imaginary part obtained by Perel' and Eliashberg [20] and model the parameter function $Q_2(k, w)$ as [11]

$$\begin{aligned} Q_2(k, w) &= \frac{A\sqrt{\omega_p^5 w(1+i)}}{\omega_2^2(k) - \omega_1^2(k)} + i \frac{\omega_2^2(k) - \omega_1^2(k)}{\nu} \\ &:= B(k)\sqrt{w(1+i)} + ih(k). \end{aligned} \quad (62)$$

Notice that (62) maintains the parity of the parameter function on the real axis:

$$Q_2(k, \omega) = B(k)\sqrt{|\omega|}[\text{sgn}(\omega) + i] + ih(k). \quad (63)$$

Observe also that by virtue of the Cauchy-Schwarz inequality (see Appendix A) $\omega_2^2 > \omega_1^2$ and that if we choose the (transport) static collision frequency ν to be equal to $\omega_p^2/4\pi\sigma_0$, we could satisfy the limiting property

$$\sigma_0 = \lim_{\omega \rightarrow 0} \lim_{k \rightarrow 0} \frac{\omega}{4\pi i} [\epsilon_{\text{MM2}}(k, \omega) - 1], \quad (64)$$

which defines the static conductivity σ_0 . Thus, the expressions (61) and (62) provide an interpolation (in the class of response functions) between the high-frequency asymptotic expansion

$$\begin{aligned} \epsilon_{\text{MM2}}^{-1}(k, w \rightarrow \infty) &\simeq 1 + \frac{\omega_p^2}{w^2} + \frac{\omega_p^2 \omega_2^2(k)}{w^4} \\ &- A \left(\frac{\omega_p}{w} \right)^{9/2} (1+i) + O\left(\frac{1}{w^{11/2}} \right) \dots, \end{aligned} \quad (65)$$

which satisfies the asymptotic form (8), and the low-frequency form (64). Note also that the real correction of the order $(\omega/\omega_p)^{-9/2}$ is negligible in (65) on the real axis with respect to other real contributions in this asymptotic expansion, while the same order imaginary contribution is the largest on the real axis (see also [71]).

As we have mentioned, it was shown in [21(a)] that $\text{Re } \nu(\omega \rightarrow \infty) \simeq \omega^{-3/2}$ in the degenerate as well as the nondegenerate plasmas. Since the asymptotic expansion of the generalized DF reads

$$\epsilon_{\text{GDL}}(0, \omega \rightarrow \infty) \simeq 1 - \frac{\omega_p^2}{\omega^2} + \frac{i\omega_p^2 \nu(\omega)}{\omega^3} - \dots,$$

we get $\text{Im } \epsilon_{\text{GDL}}(0, \omega \rightarrow \infty) \simeq \omega^{-9/2}$. Thus we point out that the generalized Drude-Lorentz model with the Born dynamic collision frequency (20) and the above BM approximation satisfy the asymptotic form (8). In addition, the interpolation form suggested in [67] for the dynamic local field correction at $T = 0$ and employed in [35] complies with it as well.

Due to the above asymptotic behavior of the DCF we cannot just replace the SCF in (62) by the static collision frequency in the Born approximation (20) $\nu(\omega)$. However, we will satisfy the asymptotic form (8) and will not modify the values of the convergent moments if we consider the model NPF

$$\begin{aligned} Q_{\text{DCF}}(k, w) &= \frac{A\sqrt{\omega_p^5 w(1+i)}}{\omega_2^2(k) - \omega_1^2(k)} \\ &+ i \frac{\omega_2^2(k) - \omega_1^2(k)}{\nu(w) + \omega_p(w\tau)^r [1 - i \tan(\pi r/2)]}, \end{aligned} \quad (66)$$

where $r \in (0, 1)$ and, for example,

$$\tau = (\beta\hbar)^{-1} = \frac{\Gamma}{\omega_p \sqrt{r_s}}$$

or just $\tau = \omega_p^{-1}$. Finally, the sum rules satisfied by the five-moment model IDF (61) are [6,7] the zeroth sum rule

$$C_0(k) = C_0^{\text{TCP}}(k) = 1 - \epsilon_{\text{TCP}}^{-1}(k, 0), \quad (67)$$

discussed in Sec. II A but with $\epsilon_{\text{TCP}}^{-1}(k, 0)$ now being the static value of the TCP IDF, the f -sum rule, and the TCP fourth loss function power moment, which takes into account the electron-ion correlations (25) [4,5]:

$$C_4(k) = C_4^{\text{TCP}}(k) = \omega_p^4 [1 + V(k) + U(k) + H]. \quad (68)$$

The presence of the correction (25) to the fourth moment implies that if we apply the Mermin model to a two-component plasma using the mixing rule [79], both SSFs $S_{ee}(q)$ and $S_{ii}(q)$ will be involved, but not the SSF $S_{ei}(q)$, which determines the H contribution to the fourth moment. Furthermore, as it was observed, precisely the latter contribution modifies the high-projectile-velocity asymptotic form of a TCP (polarization) stopping power [29,49].

2. Three-moment model vs the generalized Drude-Lorentz model

If we take into account only the moments $\{C_0(k), 0, C_2\}$, the Nevanlinna formula immediately gives for the IDF

$$\epsilon_{\text{MM1}}^{-1}(k, w) = 1 + \frac{\omega_p^2}{w^2 - \omega_1^2(k) + w Q_1(k, w)}, \quad \text{Im } w > 0. \quad (69)$$

We observe that in the long-wavelength approximation, when $\omega_1(k \rightarrow 0) \simeq \omega_p$, this expression (69) reduces to the generalized Drude-Lorentz model (19) if we choose $Q_1(k, w) = Q_1(0, w) = i v(\omega)$ and that this model is unable to incorporate the asymptotic form (8), i.e., we have that $\epsilon_{\text{MM1}}^{-1}(k, w \rightarrow \infty) \simeq 1 + \omega_p^2/w^2 + \dots$. Certainly, for a constant collision frequency or with $Q_1(k, w) = Q_1(k, w = 0) = i h(k)$, $h(k) > 0$, the fact that the loss function $\mathcal{L}_1(k, \omega) = -\text{Im } \epsilon_{\text{MM1}}^{-1}(k, \omega)/\omega$ has finite moments $\{C_0(k), 0, C_2\}$ can be easily checked by direct (analytic) integration. We have also calculated the moments of the loss function corresponding to the third-moment model IDF for two different models of the dynamic

collision frequency (see details in Sec. V A). It is clear that neither (19) nor (69) satisfies the fourth sum rule $C_4(k)$.

B. Extended TCP RPA and Mermin approximation

Let us now generalize the Mermin approximation to two-component plasmas using the mixing rule [79]

$$\epsilon_{\text{MTCP}}(k, \omega) = 1 + \frac{(\omega + i\nu)[\epsilon_{\text{RPA},e}(k, \omega + i\nu) - 1]}{\omega + i\nu \frac{\epsilon_{\text{RPA},e}(k, \omega + i\nu) - 1}{\epsilon_{\text{RPA},e}(k, 0) - 1}} + \frac{(\omega + i\nu_i)[\epsilon_{\text{RPA},i}(k, \omega + i\nu_i) - 1]}{\omega + i\nu_i \frac{\epsilon_{\text{RPA},i}(k, \omega + i\nu_i) - 1}{\epsilon_{\text{RPA},i}(k, 0) - 1}}, \quad (70)$$

where $\nu_i = \nu \sqrt{m_e/m_i}$ and for the ions we use the classical RPA DF

$$\epsilon_{\text{RPA},i}(k, w) = 1 + (k_{Di}^2/k^2) \left[1 + \frac{w}{k v_{\text{th}}} Z\left(\frac{w}{k v_{\text{th}}}\right) \right],$$

$$k_{Di}^2 = 4\pi n_i (Z n_i)^2, \quad v_{\text{th}} = \sqrt{2/\beta m_i},$$

$$Z(\zeta) = \int_{-\infty}^{\infty} \frac{ds \exp(-s^2)}{\sqrt{\pi} s - \zeta}, \quad \zeta \in \mathbb{C}, \quad \text{Im } \zeta > 0.$$

We have used the asymptotic expansions at $\omega \rightarrow \infty$, Akhiezer's theorem [3], and direct calculations to establish the following results for the TCP DF in the RPA, the extended RPA, and the above Mermin model with both the classical and extended $\epsilon_{\text{RPA},e}(k, w)$. These results are quite similar to the corresponding RPA data presented in Sec. II D. No local-field corrections were introduced to the $\epsilon_{\text{RPA},i}(k, w)$. We can now summarize our numerical results:

(i) Due to the Kramers-Kronig relations, the value of the zeroth moment is consistent with each corresponding model expression for the static IDF, but, generally speaking, we are not sure whether or not the best static DF available accounts for the system quantum-mechanical and correlation

TABLE I. The results listed in Sec. V A are complemented for each case, respectively. The values of the loss function dimensionless fourth moment $c(k_F) = C_4(k_F)/\omega_p^4$ calculated for $k = k_F$ within different models of the plasma dielectric function are displayed in columns labeled for the RPA, the extended RPA (XRPA), the Mermin model (M), the extended Born-Mermin model (XBM), and the dielectric function constructed within the moment approach (MM), while different contributions to the fourth moment defined in (31) calculated in the hypernetted-chain (HNC) approximation are presented for $k = k_F$. In the TCP cases 5–8 and within the extended Born-Mermin model the fourth moment was computed for two models of the DLFC [see Eq. (72)] and the $T = 0$ interpolation model of [67]. In the OCP cases 1–4 one observes very good agreement between the exact MM and PRA values of the moment calculated as $c(k_F) = 1 + V(k_F)$ (RPA) or $c(k_F) = 1 + V(k_F) + U(k_F)$ (XRPA), which is not the case for other models considered. The first coefficient of the asymptotic expansion of the Born DCF ν_1 defined in (50) is the magnitude of deviation of the Mermin moment from the MM value. In the TCP cases 5–8 the electron-ion contribution H is taken into account only within the moment approach; more details are provided in Sec. V A.

| Case | Γ, r_S | RPA | XRPA | M | XBM | MM | HNC: $\frac{V(k_F), U(k_F)}{\nu_1, H}$ |
|------|----------------|--------|--------|--------|-------------------------|---------|--|
| 1 | 1, 3.1545 | 5.2587 | 5.1124 | 6.1939 | 6.0473 | 5.1128 | $V = 4.2587, U = -0.1463$ |
| 2 | 1, 3.9431 | 5.1255 | 4.9792 | 6.3945 | 6.2480 | 4.9792 | $V = 4.1255, U = -0.1463$ |
| 3 | 1.0776, 2.5256 | 5.1790 | 5.0327 | 5.8135 | 5.6672 | 5.0327 | $V=4.17902, U=-0.146279$ $\nu_1=0.7579$ |
| 4 | 3.5921, 2.5256 | 3.0199 | 2.8166 | 3.7281 | 3.5248 | 2.8167 | $V=2.01991, U=-0.203236$ $\nu_1=0.7297$ |
| 5 | 1, 3.1545 | 5.2598 | 5.1815 | 6.1950 | $\frac{6.1165}{6.1086}$ | 9.5178 | $V=4.25866, U=-0.0782938$ $H=4.33743$ |
| 6 | 1, 3.9431 | 5.1266 | 5.0519 | 6.3957 | $\frac{6.3209}{6.3135}$ | 11.9288 | $V=4.1255, U=-0.07474$ $H=6.87822$ |
| 7 | 1.0776, 2.5256 | 5.1801 | 5.1187 | 5.8146 | $\frac{5.7531}{5.7540}$ | 8.4227 | $V=4.1790, U=-0.06139$ $\nu_1=0.722609, H=3.3051$ |
| 8 | 3.5921, 2.5256 | 3.0210 | 2.9931 | 3.7292 | $\frac{3.7108}{3.6966}$ | 8.2547 | $V=2.0199, U=-0.02787$ $\nu_1=0.7297, H=5.2628$ |

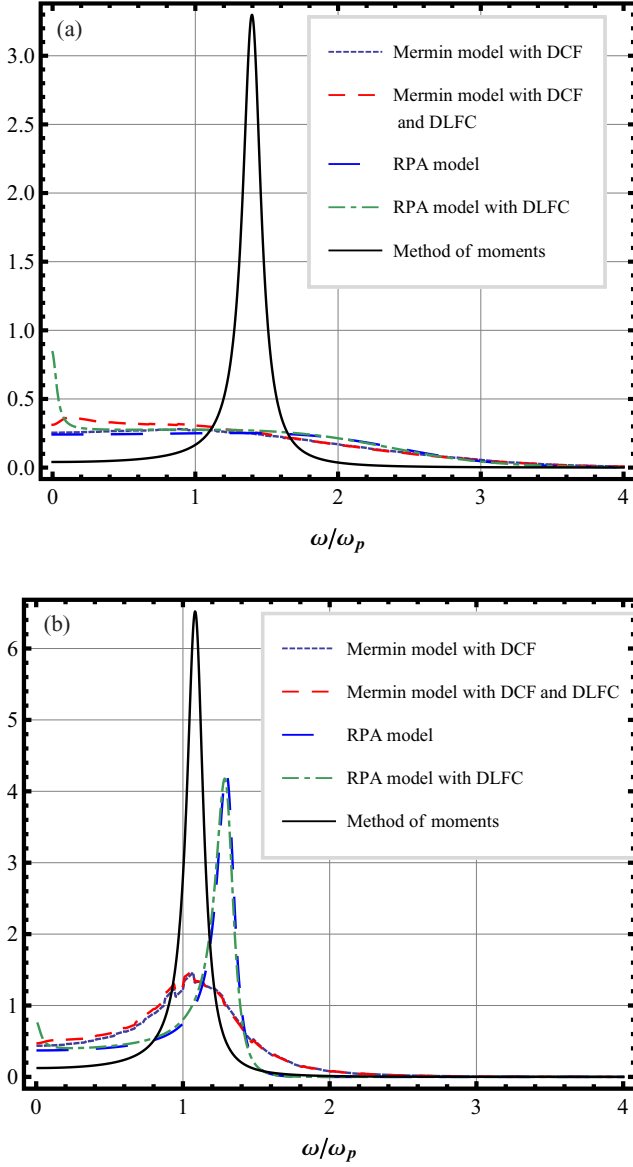


FIG. 1. (Color online) Loss function calculated for different models of an electron fluid at $\Gamma = 1$, $r_s = 3.15448$, and (a) $k = k_F$ and (b) $k = 0.7k_F$.

effects correctly. On the other hand, if the SDF is estimated as in (28), i.e., in terms of the SSF charge-charge dynamic structure factor calculated in the HNC approximation, the MM-generated forms for the IDF still satisfy this modified zeroth sum rule by construction, but the RPA, Mermin, and extended Mermin models do not.

(ii) The f -sum rule is fulfilled for all model forms of the DF or IDF we consider.

(iii) If the collision frequency ν is kept constant, the Mermin fourth moment diverges even for the extended Mermin model. Indeed, when $\omega \rightarrow \infty$, the main contribution to $\text{Im} \epsilon_{\text{MTCP}}(k, \omega)$ is still $\nu \omega_p^2 / \omega^3$, so the integrand of the fourth moment becomes constant at high frequencies.

(iv) If $\nu = \nu(k, \omega)$ is modeled as (20) or numerically, as in [31,32], the RPA value for the TCP fourth moment is recovered in the TCP RPA: $C_4^{\text{RPA TCP}}(k) = \omega_p^4 [1 + V(k)]$.

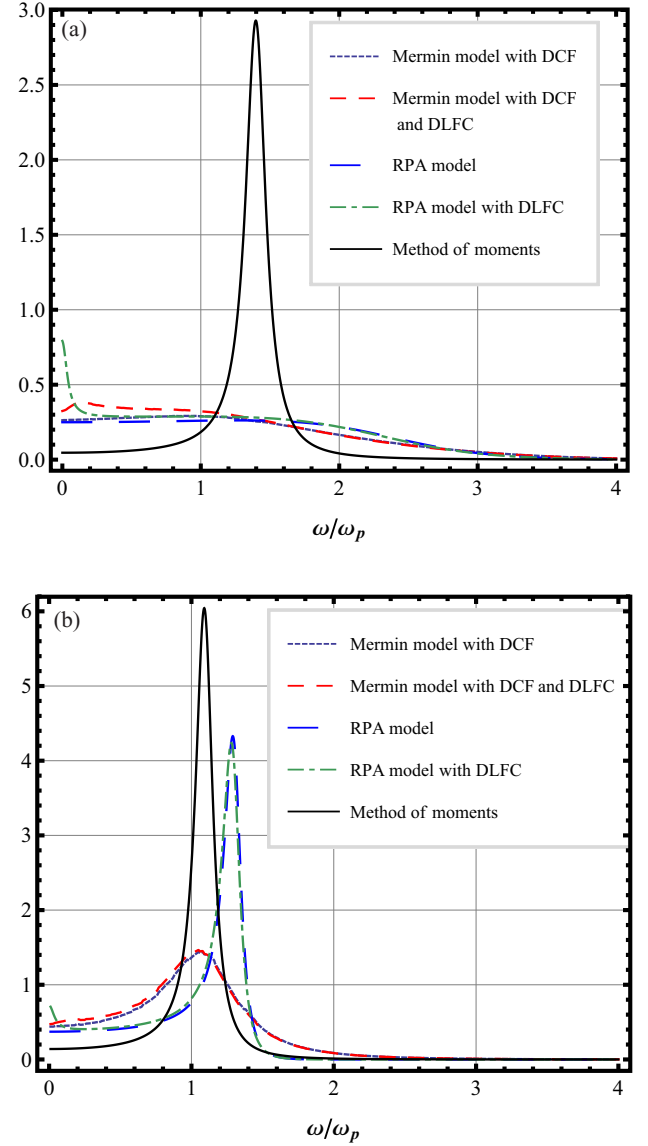


FIG. 2. (Color online) Same as in (a) Fig. 1(a) and (b) Fig. 1(b) but for $\Gamma = 1$ and $r_s = 3.9431$.

(v) If, in addition, the dynamic local-field corrections are employed in the electron contribution to the RPA DF, the fourth moment is corrected by the electron-electron contribution U ,

$$C_4^{\text{XRPA TCP}}(k) = \omega_p^4 [1 + V(k) + U(k)]. \quad (71)$$

The values for the TCP Mermin DF in the extended Mermin approximation give values that differ from those of (71). In the BM approximation this difference is very close to the dynamic collision frequency (20) first moment $i\nu_1$ imaginary part (50).

For the DLFC we have used the interpolation form [7,80]

$$G_{\text{LFC}}(q, \omega) = \frac{\nu G_{\text{LFC}}(q) + i\omega U(q)}{\nu - i\omega} \quad (72)$$

and the $T = 0$ interpolation model of [67]. Other $T \neq 0$ DLFC models might be studied, though in our computations we have

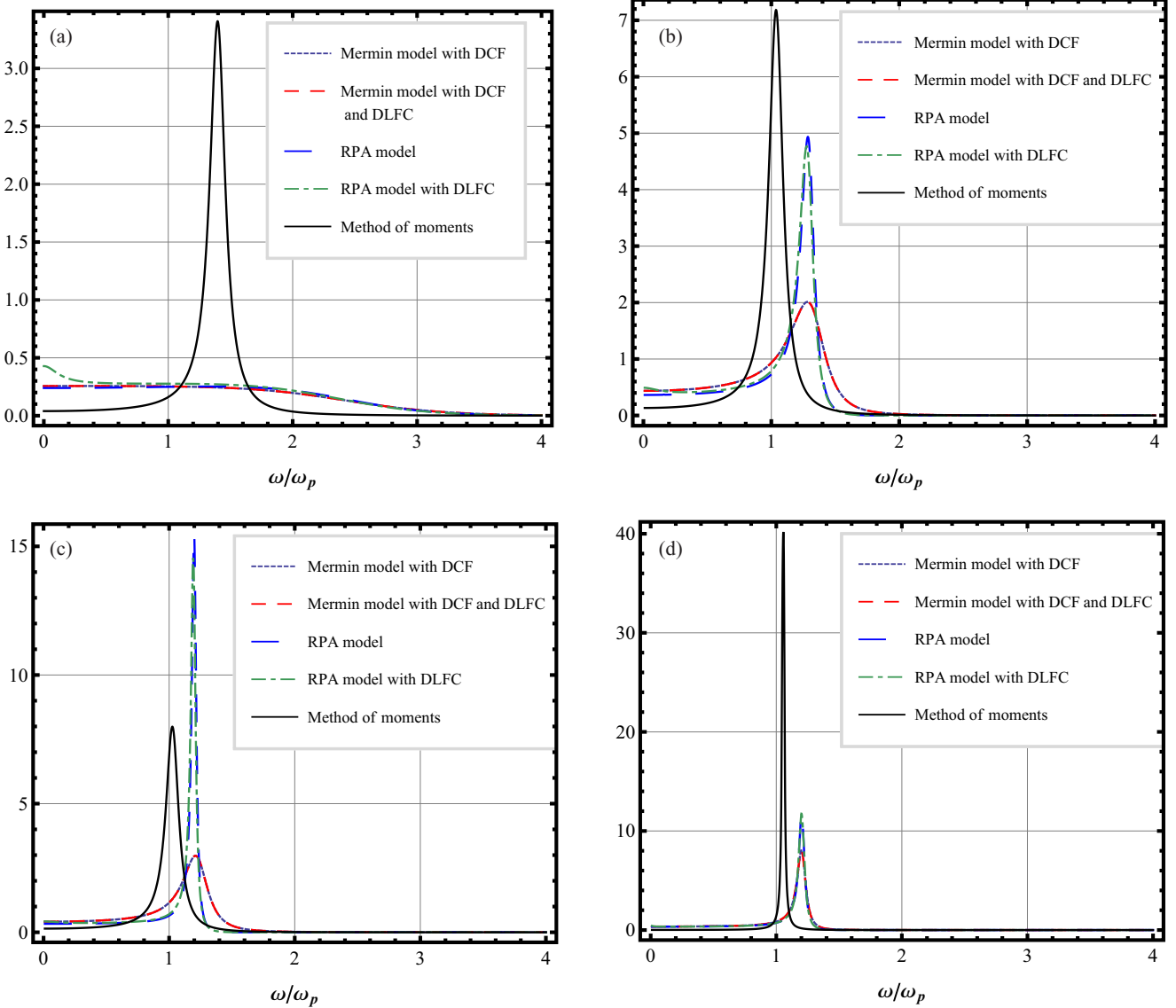


FIG. 3. (Color online) Same as in (a) Fig. 1(a) and (b) Fig. 1(b) but for $\Gamma = 1.0776$ and $r_s = 2.5256$. (c) Same as in Fig. 1(a) but for $\Gamma = 1.0776$, $r_s = 2.5256$, and $k = 0.3k_F$. (d) Same as in Fig. 1(a) but for $\Gamma = 0.10776$, $r_s = 2.5256$, and $k = 0.1k_F$.

not observed any significant dependence on the form of the DLFC employed.

(vi) Neither one of the non-MM models considered here satisfies the complete fourth sum rule (68), which includes the electron-ion contribution (25).

The above sum rules are satisfied with a rather high precision (see Sec. V A, where a small part of our numerical data is provided to support the above statements). Certainly, these data are compared to the results obtained in the MM approximation. In particular, the fourth sum rule with the electron-ion contribution H [Eq. (25)] is satisfied in the MM approximation. One has to add also that, as we have checked, the sum rules $\{C_0(k), 0, C_2, 0, C_4(k)\}$ are satisfied in the MM approximation for any Nevanlinna parameter function of the adequate mathematical class. The k dependence of $Q_2(k, \omega)$ can be specified further from the analysis of the x-ray-scattering data on the TCP collective or kinetic properties [81].

IV. STOPPING POWER

We have calculated the polarization stopping power of electron fluids and two-component plasmas for all models we have considered above and compared the results of these calculations to those obtained in the corresponding MM approximations and the asymptotic forms (21) and (24), respectively. The results are presented in detail in Sec. V B. The overall conclusions are the following.

(a) We reproduce the numerical results obtained for the stopping power of electron fluids in the papers by Barriga-Carrasco [27]. The corresponding curves that represent the dependence of the electron fluid on the projectile velocity always tend to the asymptotic form (21) from below.

(b) If we consider the stopping power of real, at least two-component completely ionized hydrogenlike plasmas, i.e., take into account the plasma ion component and the electron-ion interactions in the target plasma, the stopping

power is enhanced by them and the corresponding curves tend to the asymptotic form (24) from above.

(c) As for the polarization stopping power of the same two-component plasmas calculated within the dielectric formalism with the loss function defined as in the models considered above, such an enhancement is observed as well, but only in the expanded RPA, while in the expanded Mermin model that satisfies the fourth-moment sum rule worse than the former one, the behavior of the stopping power with respect to the modified Bethe-Larkin asymptotic form (24) is not definite.

V. NUMERICAL RESULTS

A. Values of the moments

In this section we provide some numerical data that confirm the advantages and drawbacks of the models outlined above. Certainly, we display only a small, most characteristic part of the data we have obtained.

We have calculated the values of the electron fluid and TCP loss function (1) power moments $C_0(k)$, C_2 , and $C_4(k)$ defined in (5) within the RPA (43), the extended RPA (52), the Mermin approximation (17), and the extended Mermin approximation (54). They are compared to the corresponding results obtained within the approach based on the method of moments (61). As it is known, the values of the moments are independent of the choice of the NPF $Q_2(k, w)$ from the adequate mathematical class (see Sec. III A).

In our calculations of the electron fluid power moments we have used

$$Q_2^{\text{OCP}}(k, w) = i \frac{\omega_2^2(k) - \omega_1^2(k)}{\nu} \quad (73)$$

and we have estimated the static collision frequency as it was suggested in [33],

$$\frac{\nu}{\omega_p} = 0.2387\Gamma^{3/2} \int_0^\infty \frac{dk}{k} \frac{S_{ee}(k)S_{ii}(k) - S_{ei}^2(k)}{1 + k^2\lambda_{ei}^2}, \quad (74)$$

where $\lambda_{ei} = \sqrt{\beta\hbar^2/2\pi m_e}$. In TCPs we possess additional information stemming from the asymptotic form (8). Hence, in TCPs we were able to complement the zero-frequency model expression (73) and apply the interpolation form (63).

We have pointed out that within the Mermin model (17) with a constant collision frequency ν the fourth power moment of the corresponding loss function diverges in both electron fluids and TCPs. Thus, for both types of media we have considered two cases, with the dynamic collision frequency calculated in the Born approximation (20) [in this case we were also able to calculate the parameter ν_1 of (50)] or numerically [31,32]. In electron fluids the static structure factors were found in the hypernetted approximation using the bare Coulomb potential, while in TCPs the static characteristics were determined using the Deutsch [82] (without the exchange corrections) and Kelbg (see [11] for some corrections and references) pseudopotentials.

We provide the values of different contributions to the fourth moment defined in (31) in Table I, where all results are presented for $k = k_F$. The graphs of the loss function in eight cases 1–8 are presented in Figs. 1–8 for different wave-number values, respectively. In these figures the (navy

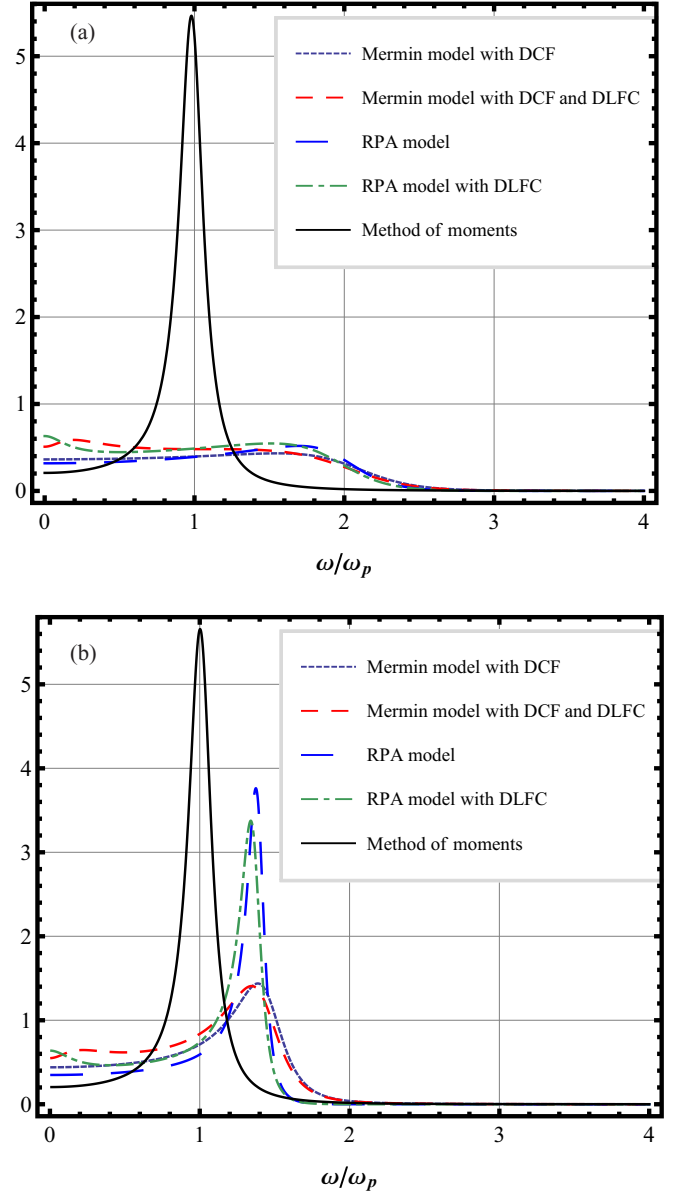


FIG. 4. (Color online) Same as in Fig. 1(a) but for (a) $\Gamma = 3.59207$ and $r_s = 2.5256$ and (b) $\Gamma = 3.59207$, $r_s = 2.5256$, and $k = 1.2k_F$.

blue) long-dashed line provides the RPA results, the (light green) dot-dashed line stands for the extended RPA data, the (navy blue) dotted line corresponds to the Mermin model, the (pink) dashed line corrections to the extended Mermin one, and the (black) solid line depicts the results of the MM approach. The dynamic collision frequency is that of [31,32] (cases 1 and 2 and cases 5 and 6, which correspond to the Figs. 1 and 2 and Figs. 5 and 6) or of (20) (the Born-Mermin model, the rest of the cases) and the DLFC is given in (72). The MM loss function proves to be physically more consistent since, due to the fluctuation-dissipation theorem, it is directly proportional to the dynamic structure factor, the form of which suggests the presence in the system of a collective Langmuir mode whose frequency is upshifted from the plasma frequency by

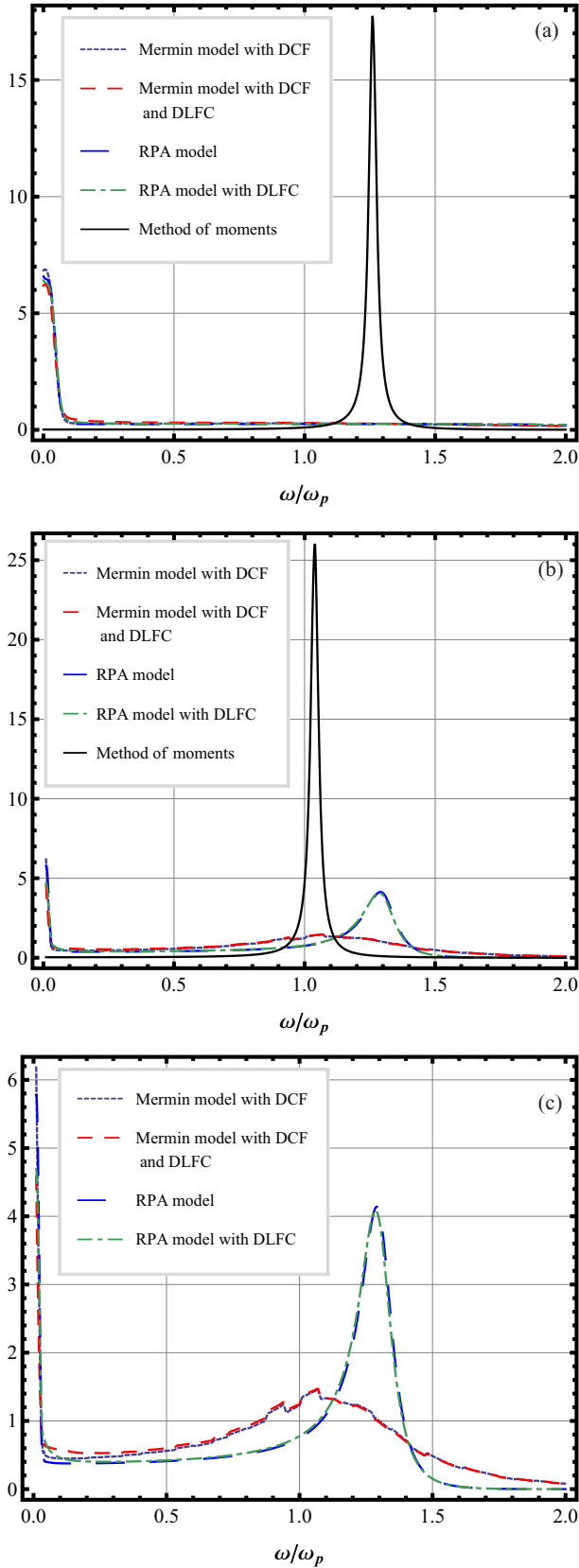


FIG. 5. (Color online) Loss function calculated for different models of a hydrogenlike plasma at $\Gamma = 1$, $r_s = 3.15448$, and (a) $k = k_F$ and (b) $k = 0.7k_F$. (c) Same in (b) but without the MM model graph.

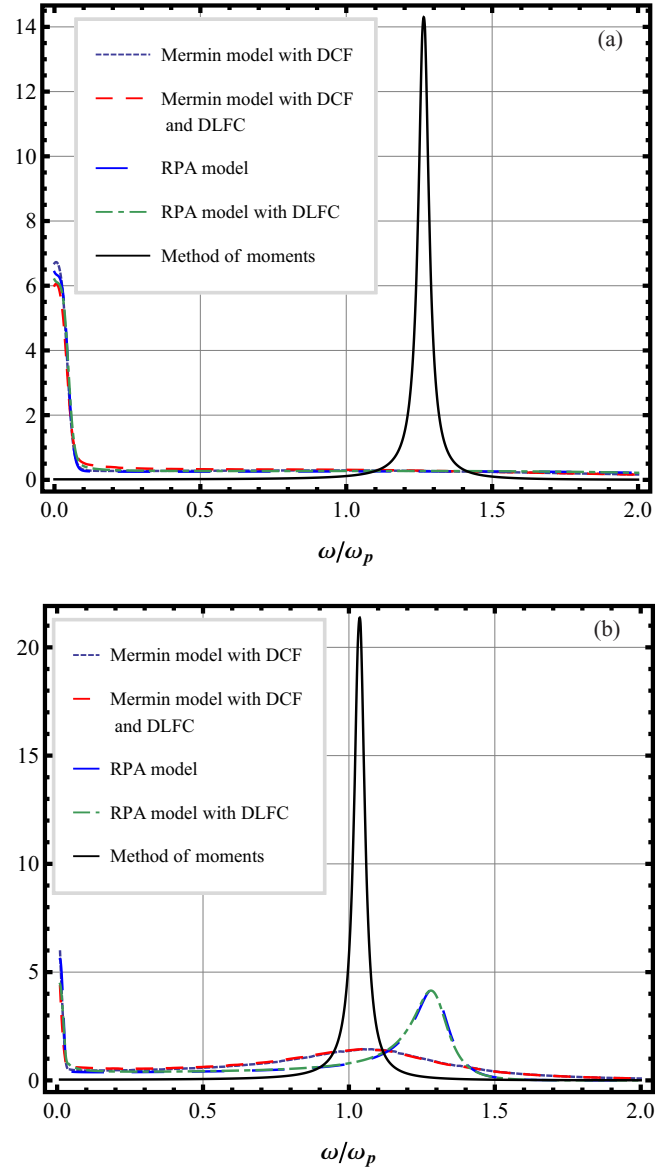


FIG. 6. (Color online) Same as in (a) Fig. 5(a) and (b) Fig. 5(b) but for $\Gamma = 1$ and $r_s = 3.9431$.

the kinetic and correlation contributions present in $\omega_2(k)$ and downshifted by the NPF real part.

1. The OCP moment values

Case 1. In the case with $T = 100\,000$ K, $r_s = 3.15448$, $D = 0.58442$, and $\Gamma = 1$ we were using the numerical data on the dynamic collision frequency (DCF) taken from [31,32] and the DLFC given in (72). Some of the graphs of the loss function are provided in Fig. 1. The theoretical value of the loss function dimensionless fourth moment $c(k_F) = C_4(k_F)/\omega_p^4$ is just $1 + V(k_F) + U(k_F) = 5.1128$, which coincides with the value of $c(k_F)$ evaluated numerically. Notice that $6.04726 - 6.19394 \approx U(k_F)$.

Case 2. In the case with $T = 80\,000$ K, $r_s = 3.9431$, $D = 0.4670$, and $\Gamma = 1$ we have again used the data from [31,32]. The results confirm the same interrelations. The graphs of the loss function are displayed in Fig. 2.

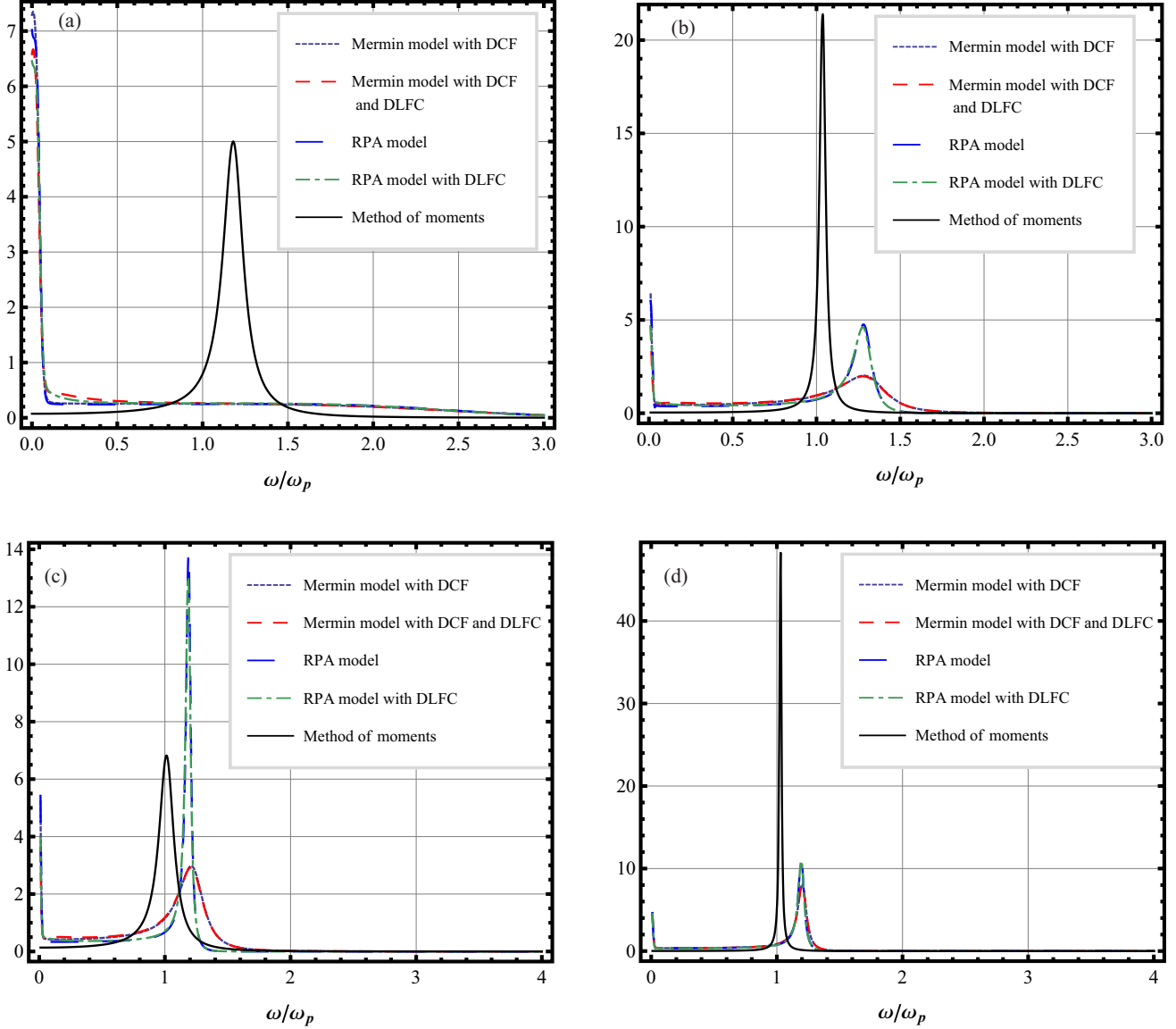


FIG. 7. (Color online) Same as in (a) Fig. 5(a) and (b) Fig. 5(b) but for $\Gamma = 1.0776$ and $r_s = 2.5256$. (c) Same in Fig. 5(a) but for $\Gamma = 1.0776$, $r_s = 2.5256$, and $k = 0.3k_F$. (d) Same as in Fig. 5(a) but for $\Gamma = 0.10776$, $r_s = 2.5256$, and $k = 0.1k_F$.

Cases 3 and 4 correspond to the Born-Mermin model with the collision frequency (20) so that we were able to estimate, in these cases, the parameter ν_1 defined in (50).

Case 3. When $T = 10$ eV, $r_s = 2.5256$, $D = 0.7858$, and $\Gamma = 1.0776$, we have that $5.17902 = 1 + V(k_F)$, $5.03273 = 1 + V(k_F) + U(k_F)$, $5.81353 \approx 5.03274 + 0.757858$, and $5.66716 \approx 5.81353 - 0.146279$.

Case 4. Finally, when $T = 3$ eV and the number density of electrons is once more equal to $n_e = 10^{23}$ cm $^{-3}$, $r_s = 2.5256$, $D = 2.61923$, and $\Gamma = 3.59207$, the values of the dimensionless moment once more verify the above interrelations with sufficient precision.

2. Values of the TCP moments

In two-component plasmas the electron contribution to (70) was estimated as in the case of the electron fluid, but the

static characteristics were calculated as we have outlined, using the Deutsch and Kelbg effective potentials, respectively. The results are quite similar to those of cases 1–4 and the conditions are, respectively, the same. The only difference is that now the electron-ion contribution to the fourth moment is present and a very good agreement between the values for this moment obtained within the MM approach and the extended RPA, i.e., using the DLFC, is violated.

Case 5. For the conditions outlined in case 1 we have that $1 + V(k_F) + U(k_F) + H = 9.517796$. Note that $6.1165 - 6.19497 \approx U(k_F)$, but $9.517796 - 5.18146 \approx H$. Additionally, the generalized Drude-Lorentz model gives in this case the value of $c(k_F) = 2.55204$.

Case 6. For the generalized Drude-Lorentz model $c(k_F) = 2.87062$.

Case 7. In this case, for the generalized Drude-Lorentz model $c(k_F) = 2.31482$.

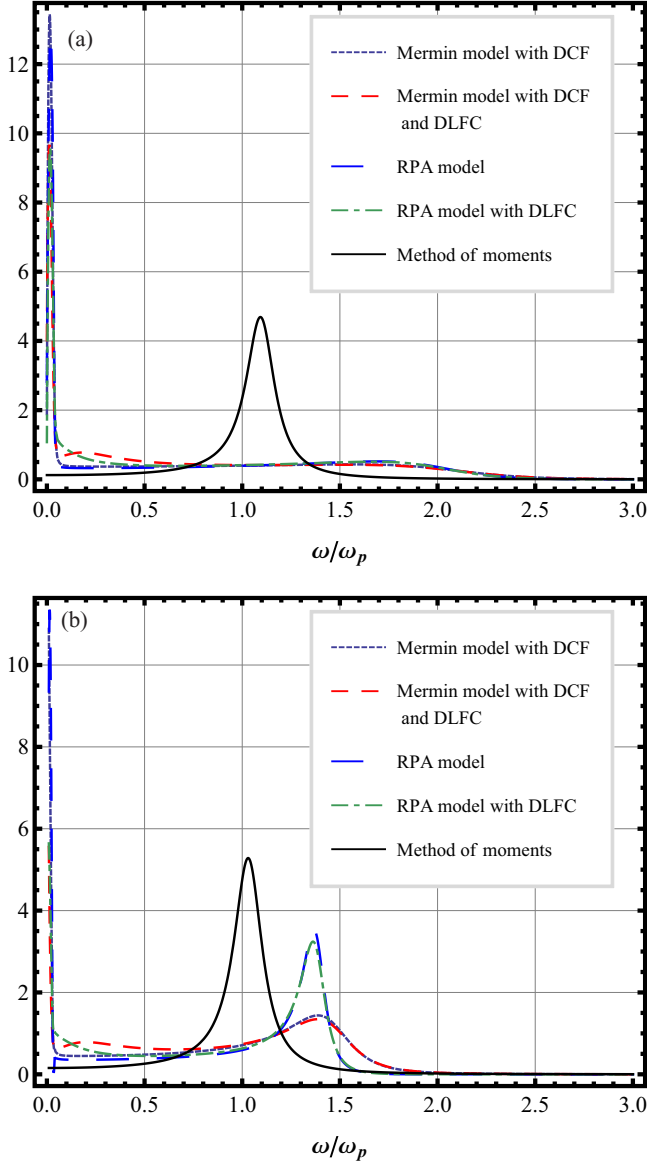


FIG. 8. (Color online) Same as in Fig. 5(a) but for (a) $\Gamma = 3.59207$ and $r_s = 2.5256$ and (b) $\Gamma = 3.59207$, $r_s = 2.5256$, and $k = 1.2k_F$.

Case 8. Now for the generalized Drude-Lorentz model $c(k_F) = 1.98331$.

The interrelations outlined above are verified in the cases 5–8 with good precision as well.

The wave-number dependence of the loss function can be observed in the figures as well. We see that the MM approach takes the collisional decay of the Langmuir mode into account at any value of the wave number, while within other models the RPA-generated singularity of the Fermi wave number persists. The position of the peak depends weakly on the model of the NPF, the contribution related to the static or dynamic collision frequency playing the decisive role. Notice also that, as expected, there is a significant decay of the Langmuir mode at $k = k_F$.

We have observed very similar results in many other cases we have considered.

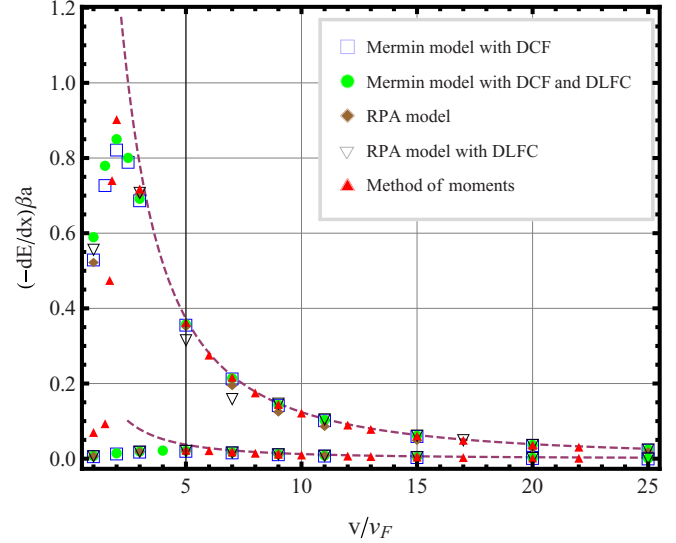


FIG. 9. (Color online) Electron fluid dimensionless polarization stopping power for different IDF models discussed in the paper for $r_s = 2.5256$. For the upper set of data $\Gamma = 10.7725$ and for the lower $\Gamma = 1.0773$. The dashed line stands for the Bethe-Larkin asymptotic form (21).

B. Stopping power data

We confirm the results of [27] (see, for example, Fig. 9). We obtain some enhancement for the stopping power when we apply the method of moments with the interpolation Nevanlinna parameter function (63) and effectively reproduce the asymptotic form (24) if we limit ourselves to the model NPF $Q_2^{\text{as}}(k, \omega) = B(k)\sqrt{|\omega|}[\text{sgn}(\omega) + i]$, while if we set $Q_2^{\text{static}}(k, \omega) = ih(k)$, the results practically coincide with those corresponding to the full $Q_2(k, \omega) = B(k)\sqrt{|\omega|}[\text{sgn}(\omega) + i] + ih(k)$. We have recalculated the TCP stopping power for the

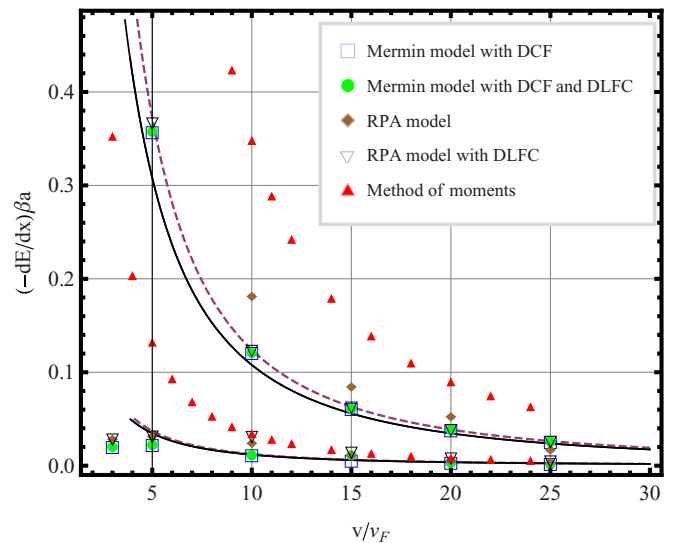


FIG. 10. (Color online) Hydrogenlike plasma stopping power for different IDF models for $r_s = 2.5256$. For the upper set of data $\Gamma = 1.07762$ and for the lower $\Gamma = 0.10776$. The solid line is the asymptotic form (24), while the (brown) dashed line stands for the Bethe-Larkin asymptote (21).

model NPF (66), but no significant changes that could be detected experimentally have been observed.

The results of alternative models of the IDF qualitatively confirm the enhancement effect (see Fig. 10). Notice that in recent studies of the TCP stopping power [83] the dielectric function was modeled in the RPA and a similar effect was observed.

VI. CONCLUSION

We have analyzed the widely used models of the unmagnetized one- and two-component completely ionized plasma longitudinal dielectric function and compared them to the one generated by the method of moments, which takes into account all known sum rules and other exact relations automatically, by construction. The advantage of the extended random-phase approximation, i.e., the RPA including two different models of the dynamic local-field correction, with respect to the Mermin and FCDF models has been pointed out. Precisely, it has been shown that in electron liquids the extended RPA satisfies all sum rules we take into account, while the Born-Mermin model deviates from the sum rule that contains the electron-electron correlation contribution. This deviation is related to the employed Born model of the dynamic collision frequency.

In two-component plasmas only the method-of-moments (inverse) dielectric function satisfies all sum rules, particularly the (fourth) sum rule, which contains, in addition to the electron-electron correlations, the contribution determined by the electron-ion static structure factor. In addition, within all models we consider, we have calculated the plasma (polarization) stopping power and have observed its enhancement in two-component systems where the electron-ion correlations in the target are taken into account. The plasma straggling [54,62] can be analyzed in the same way, but it is beyond the scope of the paper.

Our theoretical results were confirmed by numerical estimates with the plasma static characteristics evaluated in the HNC approximation. A recent model by Nersisyan *et al.* [84] from the point of view of the sum-rule approach does not go beyond the Drude-Lorentz model, i.e., it accounts for the zeroth sum rule only [see (6) and Sec. II A]. The same can be said about Ref. [83(b)]. The latter model of [84] contains two adjustment parameters and it is curious that in that work the interpolation with the static conductivity is also involved, like we do when we construct the Nevanlinna parameter function of the method of moments on the basis of an interpolation between the Perel'-Eliashberg asymptotic form of the two-component plasma dielectric function and its static conductivity. Finally, the data on the molecular-dynamics simulations of the classical stopping power [85] is interesting from a methodological point of view, but the thermodynamic conditions modeled in this work actually do not correspond to those of classical plasmas.

ACKNOWLEDGMENTS

The authors acknowledge financial support from the Science Committee of the Ministry of Education and Science of the Republic of Kazakhstan under Grants No. 1128/GF, No.

1129/GF, and No. 1099/GF. Yu.V.A. expresses gratitude for financial support provided by the Ministry by a grant "The Best Professor" and I.M.T. is grateful to the al-Farabi Kazakh National University for its hospitality. We are also grateful to I.V. Morozov for providing numerical data published in [31,32].

APPENDIX A: CAUCHY-SCHWARZ INEQUALITY IN L^2

The Cauchy-Schwarz inequality in L^2 states that

$$\left| \int_{-\infty}^{\infty} f(\omega)g(\omega)d\omega \right|^2 \leq \int_{-\infty}^{\infty} |f(\omega)|^2 d\omega \int_{-\infty}^{\infty} |g(\omega)|^2 d\omega.$$

We choose $|g(\omega)| = \sqrt{\mathcal{L}(k,\omega)/\pi}$ and $|f(\omega)| = \omega^2 \sqrt{\mathcal{L}(k,\omega)/\pi}$ to get

$$\begin{aligned} C_2^2 &= \left(\int_{-\infty}^{\infty} \omega^2 \mathcal{L}(k,\omega) \frac{d\omega}{\pi} \right)^2 \\ &\leq \left(\int_{-\infty}^{\infty} \omega^4 \mathcal{L}(k,\omega) \frac{d\omega}{\pi} \right) \\ &\quad \times \left(\int_{-\infty}^{\infty} \mathcal{L}(k,\omega) \frac{d\omega}{\pi} \right) = C_4(k)C_0(k). \end{aligned}$$

APPENDIX B: HIGH-FREQUENCY ASYMPTOTIC VALUE OF THE DLFC

Let us presume that the DLFC in an electron fluid can be chosen for the corresponding DF or rather the IDF to satisfy all five sum rules $\{C_0(k), 0, C_2, 0, C_4(k)\}$. In this case one can easily prove that the DLFC limiting value

$$G(k, \infty) = -U(k).$$

To this end it suffices to compare the expressions

$$\epsilon_{\text{XRPA}}^{-1}(k, w) = 1 - \frac{\phi(k)\Pi(k, w)}{1 - \phi(k)[1 - G(k, w)]\Pi(k, w)} \quad (\text{B1})$$

and (61):

$$\begin{aligned} &\frac{\phi(k)\Pi(k, w)}{\phi(k)[1 - G(k, w)]\Pi(k, w) - 1} \\ &= \frac{\omega_p^2[w + Q_2(k, w)]}{w(w^2 - \omega_2^2) + Q_2(k, w)(w^2 - \omega_1^2)}. \end{aligned} \quad (\text{B2})$$

Then the electron fluid DLFC and the (five-moment) Nevanlinna parameter function $Q_2(k, w)$ can be interrelated directly:

$$\frac{Q_2(k, w)}{w} = -\frac{R_2(k, w) + G(k, w)}{R_1(k, w) + G(k, w)}, \quad (\text{B3})$$

where

$$R_j(k, w) = \frac{w^2 - \omega_j^2(k)}{\omega_p^2} + \frac{1}{\phi(k)\Pi(k, w)} - 1, \quad j = 1, 2.$$

Further, we take into account the asymptotic form of the RPA polarization operator

$$\Pi(k, w \rightarrow \infty) \simeq -\frac{\omega_p^2}{\phi(k)w^2} \left[1 + \frac{\omega_p^2}{w^2} V(k) + O\left(\left(\frac{kv_F}{w}\right)^4\right) \right], \quad (\text{B4})$$

which is equivalent to (45), and find the limiting value of (B3) when $w \rightarrow \infty$:

$$\lim_{w \rightarrow \infty} \frac{Q_2(k, w)}{w} = \frac{\omega_p^2 [G(k, \infty) + U(k)]}{\omega_2^2(k) - \omega_1^2(k) - \omega_p^2 [G(k, \infty) + U(k)]}. \quad (\text{B5})$$

We know that along any ray in the upper half plane $\text{Im } w > 0$, $\lim_{w \rightarrow \infty} Q_2(k, w)/w = 0$, and $\omega_2^2(k) - \omega_1^2(k) > 0$ for any finite wave-number value, hence $G(k, \infty) = -U(k)$. This general result implies that the influence of the self-energy contribution to the system average kinetic energy with correlations [73] is negligible, at least if we assume that the extended RPA model loss function can possess all five convergent moments.

-
- [1] S. H. Glenzer *et al.*, *Plasma Phys. Control. Fusion* **54**, 045013 (2012); S. H. Glenzer, Book of Abstracts of the 14th International Conference on the Physics of Non-Ideal Plasmas, Rostock, 2012 (unpublished), p. 28.
- [2] M. G. Kreĭn and A. A. Nudel'man, *The Markov Moment Problem and Extremal Problems*, Translations of Mathematical Monographs Vol. 50 (American Mathematical Society, Providence, 1977).
- [3] N. I. Akhiezer, *The Classical Moment Problem* (Hafner, New York, 1965).
- [4] V. M. Adamyān, T. Meyer, and I. M. Tkachenko, *Sov. J. Plasma Phys.* **11**, 481 (1985).
- [5] V. M. Adamyān and I. M. Tkachenko, *Contrib. Plasma Phys.* **43**, 252 (2003).
- [6] Y. V. Arkhipov, A. Askaruly, D. Ballester, A. E. Davletov, G. M. Meirkanova, and I. M. Tkachenko, *Phys. Rev. E* **76**, 026403 (2007).
- [7] Y. V. Arkhipov, A. Askaruly, D. Ballester, A. E. Davletov, I. M. Tkachenko, and G. Zwicknagel, *Phys. Rev. E* **81**, 026402 (2010).
- [8] I. M. Tkachenko, Y. V. Arkhipov, and A. Askaruly, *The Method of Moments and its Applications in Plasma Physics* (Lambert, Saarbrücken, 2012).
- [9] J. Vorberger, Z. Donko, I. M. Tkachenko, and D. O. Gericke, *Phys. Rev. Lett.* **109**, 225001 (2012).
- [10] K. I. Golden and G. J. Kalman, *Phys. Rev. E* **88**, 033107 (2013).
- [11] Y. V. Arkhipov, A. B. Ashikbayeva, A. Askaruly, A. E. Davletov, and I. M. Tkachenko, *Contrib. Plasma Phys.* **53**, 375 (2013).
- [12] N. D. Mermin, *Phys. Rev. B* **1**, 2362 (1970).
- [13] K. Morawetz and U. Fuhrmann, *Phys. Rev. E* **62**, 4382 (2000); **61**, 2272 (2000).
- [14] G. S. Atwal and N. W. Ashcroft, *Phys. Rev. B* **65**, 115109 (2002); **67**, 233104 (2003).
- [15] J. Lindhard, K. Dan. Vidensk. Selsk. Mat. Fys. Medd. **28**, 1 (1954).
- [16] O. V. Dolgov, D. A. Kirzhnits, and E. G. Maksimov, *Rev. Mod. Phys.* **53**, 81 (1981).
- [17] E. G. Maksimov and O. V. Dolgov, *Usp. Fiz. Nauk* **177**, 983 (2007) [*Sov. Phys. Usp.* **50**, 933 (2007)].
- [18] S. Ichimaru, *Statistical Plasma Physics* (Addison-Wesley, New York, 1991), Vol. 1.
- [19] S. Ichimaru, *Statistical Plasma Physics: Condensed Plasmas* (Addison-Wesley, New York, 1994), Vol. 2.
- [20] V. I. Perel' and G. M. Eliashberg, *Zh. Eksp. Teor. Fiz.* **41**, 886 (1961) [*Sov. Phys. JETP* **14**, 633 (1962)].
- [21] (a) H. Reinholz, R. Redmer, G. Röpke, and A. Wierling, *Phys. Rev. E* **62**, 5648 (2000); (b) A. Selchow, G. Röpke, A. Wierling, H. Reinholz, T. Pschiwul, and G. Zwicknagel, *ibid.* **64**, 056410 (2001).
- [22] (a) I. M. Tkachenko, in 33rd International Workshop on Physics of HED in Matter, Hirschegg, 2013 (unpublished); (b) V. M. Adamyān and I. M. Tkachenko, *Operator Theory: Advances and Applications* (Birkhauser, Basel, 2000), Vol. 33, p. 118; (c) G. Kalman and K. I. Golden, *Phys. Rev. A* **29**, 844 (1984).
- [23] K. Morawetz, *Phys. Rev. B* **66**, 075125 (2002).
- [24] A. K. Das, *J. Phys. F* **5**, 2035 (1975).
- [25] C. Gouedard and C. Deutsch, *J. Math. Phys.* **19**, 32 (1978).
- [26] N. R. Arista and W. Brandt, *Phys. Rev. A* **29**, 1471 (1984).
- [27] (a) M. D. Barriga-Carrasco, *Phys. Rev. E* **73**, 026401 (2006); (b) **76**, 016405 (2007); (c) **79**, 027401 (2009); (d) **82**, 046403 (2010).
- [28] D. Casas, M. D. Barriga-Carrasco, and J. Rubio, *Phys. Rev. E* **88**, 033102 (2013).
- [29] D. Ballester and I. M. Tkachenko, *Phys. Rev. Lett.* **101**, 075002 (2008).
- [30] R. Thiele, P. Sperling, M. Chen, T. Bornath, R. R. Fäustlin, C. Fortmann, S. H. Glenzer, W.-D. Kraeft, A. Pukhov, S. Toleikis, T. Tschentscher, and R. Redmer, *Phys. Rev. E* **82**, 056404 (2010).
- [31] H. Reinholz, I. Morozov, G. Röpke, and T. Millat, *Phys. Rev. E* **69**, 066412 (2004).
- [32] I. Morozov, H. Reinholz, G. Röpke, A. Wierling, and G. Zwicknagel, *Phys. Rev. E* **71**, 066408 (2005).
- [33] M. Baus, J.-P. Hansen, and L. Sjögren, *Phys. Lett.* **82A**, 180 (1981).
- [34] A. Esser, R. Redmer, and G. Röpke, *Contrib. Plasma Phys.* **43**, 33 (2003).
- [35] C. Fortmann, A. Wierling, and G. Röpke, *Phys. Rev. E* **81**, 026405 (2010).
- [36] J.-P. Hansen and I. R. McDonald, *Theory of Simple Liquids* (Academic, New York, 1976).
- [37] J. Hong and M. H. Lee, *Phys. Rev. Lett.* **55**, 2375 (1985); J. Hong and C. Kim, *Phys. Rev. A* **43**, 1965 (1991).
- [38] G. Kalman and K. I. Golden, *Phys. Rev. A* **41**, 5516 (1990); K. I. Golden, G. Kalman, and P. Wynn, *ibid.* **46**, 3454 (1992).
- [39] A. V. Filippov, A. N. Starostin, I. M. Tkachenko, and V. E. Fortov, *Phys. Lett. A* **376**, 31 (2011).
- [40] K. Morawetz, U. Fuhrmann, and R. Walke, *Nucl. Phys. A* **649**, 348 (1999).
- [41] H. Bethe, *Ann. Phys. (Leipzig)* **5**, 325 (1930).
- [42] A. I. Larkin, *Zh. Eksp. Teor. Fiz.* **37**, 264 (1959) [*Sov. Phys. JETP* **37**, 186 (1960)].
- [43] F. C. Young, D. Mosher, S. J. Stephanakis, S. A. Goldstein, and T. A. Mehlhorn, *Phys. Rev. Lett.* **49**, 549 (1982).
- [44] G. Belyaev, M. Basko, A. Cherkasov, A. Golubev, A. Fertman, I. Roudskoy, S. Savin, B. Sharkov, V. Turtikov, A. Arzumanov, A. Borisenko, I. Goralchev, S. Lysukhin, D. H. H. Hoffmann, and A. Tauschwitz, *Phys. Rev. E* **53**, 2701 (1996).

- [45] A. Golubev *et al.*, *Phys. Rev. E* **57**, 3363 (1998).
- [46] A. D. Fertman, T. Y. Mutin, M. M. Basko, A. A. Golubev, T. V. Kulevoy, R. P. Kuybeda, V. I. Pershin, I. V. Roudskoy, and B. Y. Sharkov, *Nucl. Instrum. Methods Phys. Res. Sect. B* **247**, 199 (2006).
- [47] D. O. Gericke, M. Schlanges, and T. Bornath, *Phys. Rev. E* **65**, 036406 (2002).
- [48] S. Y. Gus'kov, V. B. Rozanov, N. V. Zmitrenko, D. V. Il'in, A. A. Levkovskii, and V. E. Sherman, *Fiz. Plazmy* **35**, 771 (2009) [*Plasma Phys. Rep.* **35**, 709 (2009)].
- [49] D. Ballester and I. M. Tkachenko, *J. Phys. A: Math. Theor.* **42**, 214035 (2009).
- [50] V. B. Mintsev *et al.*, in Book of Abstracts of the 14th International Conference on the Physics of Non-Ideal Plasmas Rostock, 2012 (Ref. [1]), p. 31.
- [51] B. Vauzour *et al.*, *Phys. Rev. Lett.* **109**, 255002 (2012).
- [52] Y. V. Arhipov, A. B. Ashikbayeva, A. Askaruly, A. E. Davletov, and I. M. Tkachenko, *Europhys. Lett.* **104**, 35003 (2013).
- [53] E. Fermi and E. Teller, *Phys. Rev.* **72**, 399 (1947).
- [54] N. R. Arista and W. Brandt, *Phys. Rev. A* **23**, 1898 (1981).
- [55] W. D. Kraeft and B. Strege, *Physica A* **149**, 313 (1988).
- [56] A. Bret and C. Deutsch, *Phys. Rev. E* **48**, 2994 (1993).
- [57] K. Morawetz and G. Röpke, *Phys. Rev. E* **54**, 4134 (1996).
- [58] J. Ortner and I. M. Tkachenko, *Phys. Rev. E* **63**, 026403 (2001).
- [59] W. H. Barkas, J. N. Dyer, and H. H. Heckman, *Phys. Rev. Lett.* **11**, 26 (1963).
- [60] D. Gardes, A. Servajean, B. Kubica, C. Fleurier, D. Hong, C. Deutsch, and G. Maynard, *Phys. Rev. A* **46**, 5101 (1992).
- [61] N. R. Arista, *J. Phys. C* **18**, 5127 (1985).
- [62] G. Maynard and C. Deutsch, *Phys. Rev. A* **26**, 665 (1982).
- [63] X.-Z. Yan, S. Tanaka, S. Mitake, and S. Ichimaru, *Phys. Rev. A* **32**, 1785 (1985).
- [64] S. Tanaka and S. Ichimaru, *J. Phys. Soc. Jpn.* **54**, 2537 (1985).
- [65] I. Nagy, J. László, and J. Giber, *Z. Phys. A* **321**, 221 (1985).
- [66] I. Nagy, A. Arnau, and P. M. Echenique, *Phys. Rev. B* **48**, 5650 (1993).
- [67] B. Dabrowski, *Phys. Rev. B* **34**, 4989 (1986).
- [68] D. O. Gericke, M. Schlanges, and W. D. Kraeft, *Phys. Lett. A* **222**, 241 (1996).
- [69] Y. V. Arkipov, F. B. Baimbetov, A. E. Davletov, and K. V. Starikov, *Plasma Phys. Control. Fusion* **42**, 455 (2000); *Phys. Scr.* **63**, 194 (2001).
- [70] I. Z. Fisher, *Statistical Theory of Liquids* (University of Chicago Press, Chicago, 1964).
- [71] V. M. Adamyany and I. M. Tkachenko, *High Temp.* **21**, 307 (1983) [*Sov. Phys. Teplofiz. Vys. Temp.* **21**, 417 (1983)]; M. J. Corbatón and I. M. Tkachenko, Book of Abstracts of the International Conference on Strongly Coupled Coulomb Systems, Camerino, 2008 (unpublished), p. 90.
- [72] A. A. Abrikosov, L. P. Gorkov, and I. E. Dzyaloshinski, *Methods of Quantum Field Theory in Statistical Physics* (Pergamon, Oxford, 1965).
- [73] A. A. Kugler, *J. Stat. Phys.* **12**, 35 (1975).
- [74] J. D. Huba, *Revised NRL Plasma Formulary* (NRL, Washington, DC, 2002), p. 30.
- [75] B. D. Fried and S. D. Conte, *The Plasma Dispersion Function* (Academic, New York, 1961).
- [76] I. M. Tkachenko, J. Ortner, and J. Alcober, *J. Phys. IV* **10**, 195 (2000).
- [77] I. M. Tkachenko, in *Book of Abstracts of the International Conference on Operator Theory and its Applications in Mathematical Physics* (Stefan Banach International Mathematical Center, Będlewo, 2002), p. 20.
- [78] D. Varentsov, I. M. Tkachenko, and D. H. H. Hoffmann, *Phys. Rev. E* **71**, 066501 (2005).
- [79] G. Röpke, A. Selchow, A. Wierling, and H. Reinholz, *Phys. Lett. A* **260**, 365 (1999); C. Deutsch *et al.*, *Nucl. Instrum. Methods Phys. Res. Sect. A* **733**, 39 (2014).
- [80] S. Tanaka and S. Ichimaru, *Phys. Rev. A* **35**, 4743 (1987).
- [81] S. H. Glenzer and R. Redmer, *Rev. Mod. Phys.* **81**, 1625 (2009).
- [82] C. Deutsch, *Phys. Lett. A* **60**, 317 (1977); C. Deutsch, M.-M. Gombert, and H. Minoo, *ibid.* **66**, 381 (1978); **72**, 481 (1979).
- [83] (a) C. Deutsch and P. Fromy, *J. Plasma Phys.* **79**, 391 (2013); (b) P. K. Shukla and M. Akbari-Moghanjoughi, *Phys. Rev. E* **87**, 043106 (2013).
- [84] H. B. Nersisyan, M. E. Veysman, N. E. Andreev, and H. H. Matevosyan, *Phys. Rev. E* **89**, 033102 (2014).
- [85] P. E. Grabowski, M. P. Surh, D. F. Richards, F. R. Graziani, and M. S. Murillo, *Phys. Rev. Lett.* **111**, 215002 (2013).